

# CHROMIUM OXIDE CATALYSTS IN THE DEHYDROGENATION OF ALKANES

Sanna Airaksinen



TEKNILLINEN KORKEAKOULU  
TEKNISKA HÖGSKOLAN  
HELSINKI UNIVERSITY OF TECHNOLOGY  
TECHNISCHE UNIVERSITÄT HELSINKI  
UNIVERSITE DE TECHNOLOGIE D'HELSINKI

## CHROMIUM OXIDE CATALYSTS IN THE DEHYDROGENATION OF ALKANES

Sanna Airaksinen

Dissertation for the degree of Doctor of Science in Technology to be presented with due permission of the Department of Chemical Technology for public examination and debate in Auditorium Ke 2 (Komppa Auditorium) at Helsinki University of Technology (Espoo, Finland) on the 21st of October, 2005, at 12 o'clock noon.

Helsinki University of Technology  
Department of Chemical Technology  
Laboratory of Industrial Chemistry

Teknillinen korkeakoulu  
Kemian tekniikan osasto  
Teknillisen kemian laboratorio

Distribution:

Helsinki University of Technology

Laboratory of Industrial Chemistry

P. O. Box 6100

FI-02015 HUT

Tel. +358-9-4511

Fax. +358-9-451 2622

E-Mail: arja.tuohino@tkk.fi

© Sanna Airaksinen

ISBN 951-22-7795-6 (print), 951-22-7796-4 (pdf, available at <http://lib.tkk.fi/Diss/>)  
ISSN 1235-6840

Otamedia Oy  
Espoo 2005

## ABSTRACT

Light alkenes, such as propene and butenes, are important intermediates in the manufacture of fuel components and chemicals. The direct catalytic dehydrogenation of the corresponding alkanes is a selective way to produce these alkenes and is frequently carried out using chromia/alumina catalysts. The aim of this work was to obtain structure–activity information, which could be utilised in the optimisation of this catalytic system. The properties of chromia/alumina catalysts were investigated by advanced in situ and ex situ spectroscopic methods, and the activities were measured in the dehydrogenation of isobutane.

The dehydrogenation activity of chromia/alumina was attributed to coordinatively unsaturated redox and non-redox  $\text{Cr}^{3+}$  ions at all chromium loadings. In addition, the oxygen ions in the catalyst appeared to participate in the reaction. The reduction of chromia/alumina resulted in formation of adsorbed surface species: hydroxyl groups bonded to chromia and alumina were formed in reduction by hydrogen and alkanes, and carbon-containing species in reduction by carbon monoxide and alkanes. Prereduction with hydrogen or carbon monoxide decreased the dehydrogenation activity. The effect by hydrogen was suggested to be related to the amount of OH/H species on the reduced surface affecting the number of coordinatively unsaturated chromium sites, and the effect by carbon monoxide to the formation of unselective chromium sites and carbon-containing species.

The chromia/alumina catalysts were deactivated with time on stream and in cycles of (pre)reduction–dehydrogenation–regeneration. The deactivation with time on stream was caused mainly by coke formation. The nature of the coke species changed during dehydrogenation. Carboxylates and aliphatic hydrocarbon species formed at the beginning of the reaction and unsaturated/aromatic hydrocarbons and graphite-like species with increasing time on stream. The deactivation in several dehydrogenation–regeneration cycles was attributed to a decrease in the number of active sites, which was possibly caused by clustering of the active phase into more three-dimensional structures.

Acidic hydroxyl species of exposed alumina support may have contributed to the side reactions observed during dehydrogenation. Chromium catalysts prepared on unmodified alumina and on alumina modified with basic aluminium nitride-type species were compared in an attempt to increase the activity and selectivity in dehydrogenation. However, the presence of nitrogen in the catalyst was not beneficial for the dehydrogenation activity.

A kinetic model was derived for the rate of dehydrogenation of isobutane on chromia/alumina. The dehydrogenation results were best described by a model with isobutane adsorption, possibly on a pair of chromium and oxygen ions, as the rate-determining step. Satisfactory description of the reaction rate depended upon inclusion of the isobutene and hydrogen adsorption parameters in the mathematical model. The activation energy of the rate-determining step was estimated to be  $137 \pm 5$  kJ/mol.

## PREFACE

The work for this thesis was carried out in the Laboratory of Industrial Chemistry at Helsinki University of Technology between 1999 and 2004, and in the Instituto de Catálisis y Petroleoquímica, CSIC, Madrid, Spain between May and June 2003. Funding from the Academy of Finland is gratefully acknowledged. Additional support was received from the European Science Foundation through COST Action D15.

I am most grateful to my supervisor, Professor Outi Krause for her advice, continuous support and interest for this work. Warm thanks are due to my co-authors Dr. Miguel A. Bañares, Dr. Elina Harlin, Dr. Riikka Puurunen, Dr. Jaana Kanervo, Dr. Jouko Lahtinen, Mr. Jani Sainio, Dr. Olga Guerrero-Pérez and Professor Kuei-jung Chao for their co-operation and help in the research. I would especially like to thank Dr. Elina Harlin for getting me started with my postgraduate studies and Dr. Miguel A. Bañares for giving me the opportunity to carry out research work at the Instituto de Catálisis y Petroleoquímica.

Dr. Arla Kytökivi and Ms. Mirja Rissanen are thanked for the preparation of the ALD chromia/alumina samples, and Ms. Johanna Lempiäinen, Mr. Markus Jönsson and Ms. Satu Korhonen for their help with some of the experiments. The participants in the project “Kinetic Modeling of C<sub>3</sub>–C<sub>5</sub> Alkanes”, funded by the Academy of Finland, and in the working group 0021-01 of the European Science Foundation COST Action D15 are thanked for the ideas and valuable discussions we have shared. My colleagues at the Laboratory of Industrial Chemistry are thanked for creating a pleasant and motivating work atmosphere.

My warmest thanks go to my family for their support, and to Esa for his help, understanding and patience.

Vantaa, February 2005

Sanna Airaksinen

## LIST OF PUBLICATIONS

This thesis is based on the following appended publications, which are referred to in the text by their Roman numerals:

- I Puurunen, R. L., Airaksinen, S. M. K., Krause, A. O. I., Chromium(III) Supported on Aluminum-Nitride-Surfaced Alumina: Characteristics and Dehydrogenation Activity, *J. Catal.* **213** (2003) 281–290.
- II Airaksinen, S. M. K., Krause, A. O. I., Sainio, J., Lahtinen, J., Chao, K.-j., Guerrero-Pérez, M. O., Bañares, M. A., Reduction of Chromia/Alumina Catalyst Monitored by DRIFTS-Mass Spectrometry and TPR-Raman Spectroscopy, *Phys. Chem. Chem. Phys.* **5** (2003) 4371–4377.
- III Airaksinen, S. M. K., Bañares, M. A., Krause, A. O. I., In Situ Characterisation of Carbon-Containing Species Formed on Chromia/Alumina during Propane Dehydrogenation, *J. Catal.* **230** (2005) 507–513.
- IV Airaksinen, S. M. K., Krause, A. O. I., Effect of Catalyst Prereduction on the Dehydrogenation of Isobutane over Chromia/Alumina, *Ind. Eng. Chem. Res.* **44** (2005) 3862–3868.
- V Airaksinen, S. M. K., Kanervo, J. M., Krause, A. O. I., Deactivation of  $\text{CrO}_x/\text{Al}_2\text{O}_3$  Catalysts in the Dehydrogenation of *i*-Butane, *Stud. Surf. Sci. Catal.* **136** (2001) 153–158.
- VI Airaksinen, S. M. K., Harlin, M. E., Krause, A. O. I., Kinetic Modeling of Dehydrogenation of Isobutane on Chromia/Alumina Catalyst, *Ind. Eng. Chem. Res.* **41** (2002) 5619–5626.

The author's contribution to the appended publications:

- I, V She made the research plan for the dehydrogenation part, carried out the dehydrogenation experiments and interpreted their results. She wrote the manuscript together with the co-authors.
- II She made the research plan together with the co-authors, carried out the in situ DRIFTS experiments, interpreted their results and wrote the manuscript.
- III She made the research plan, carried out the experiments, interpreted the results of the in situ DRIFTS measurements and wrote the manuscript.
- IV She made the research plan, carried out or supervised the experiments, interpreted the results and wrote the manuscript.
- VI She made the research plan together with the co-authors, carried out the experiments, interpreted the results and wrote the manuscript.

# CHROMIUM OXIDE CATALYSTS IN THE DEHYDROGENATION OF ALKANES

<b>ABSTRACT .....</b>	<b>1</b>
<b>PREFACE .....</b>	<b>2</b>
<b>LIST OF PUBLICATIONS .....</b>	<b>3</b>
<b>1 INTRODUCTION .....</b>	<b>7</b>
1.1 Industrial dehydrogenation in production of light alkenes.....	7
1.2 Scope of the research.....	9
<b>2 SUPPORTED CHROMIA CATALYSTS.....</b>	<b>11</b>
2.1 Oxidised chromia catalysts.....	11
2.2 Reduced chromia catalysts .....	13
<b>3 EXPERIMENTAL .....</b>	<b>15</b>
3.1 Preparation and characterisation of catalysts.....	15
3.2 In situ spectroscopic measurements .....	18
3.3 Dehydrogenation activity measurements .....	19
3.4 Kinetic modelling of isobutane dehydrogenation.....	19
<b>4 RESULTS AND DISCUSSION.....</b>	<b>21</b>
4.1 Chromium catalysts supported on aluminium nitride-modified alumina.....	21
4.1.1 Chemisorption of Cr(acac) <sub>3</sub> .....	21
4.1.2 Activity in dehydrogenation .....	22
4.2 Reduction of chromia/alumina .....	24
4.2.1 Reduction measurements.....	25
4.2.2 Structural changes during reduction.....	25
4.2.3 Surface species formed during reduction .....	26
4.3 Calcined and prereduced chromia/alumina in dehydrogenation .....	31
4.3.1 Activity in dehydrogenation .....	31
4.3.2 Surface species formed during dehydrogenation.....	32
4.3.3. Considerations on the effect of prereduction.....	35

4.4	Deactivation of ALD-prepared and fluidised bed chromia/alumina .....	37
4.4.1	Behaviour with time on alkane stream .....	37
4.4.2	Behaviour in cycles of (pre)reduction–dehydrogenation–regeneration .	40
4.5	Kinetic model for isobutane dehydrogenation.....	43
<b>5</b>	<b>SUMMARY .....</b>	<b>47</b>
	<b>NOMENCLATURE .....</b>	<b>50</b>
	<b>REFERENCES .....</b>	<b>52</b>

## **APPENDICES**

Publications I–VI

# 1 INTRODUCTION

## 1.1 Industrial dehydrogenation in production of light alkenes

Light alkenes, propene and butenes, are important intermediates in the manufacture of polymers, chemicals and fuel components. Propene and butenes are primarily produced as coproducts in catalytic and steam cracking processes. For example, 67% of the total amount of propene produced in 2003 (57.6 million tons) was obtained as coproduct in ethene manufacture by steam cracking processes [1]. In 1997, butenes were produced in the amount of 31 million tons principally by catalytic cracking and steam cracking [2]. Demand for propene is dominated by the polypropylene industry; other uses for propene include the production of acrylic acid, acrylonitrile, cumene, oxo-alcohols and propylene oxide [1]. Butenes are mainly used in the manufacture of fuel components such as alkylates and oxygenates [2].

In addition to the cracking processes, light alkenes can also be obtained by other methods. Catalytic dehydrogenation of alkanes is a selective way to produce alkenes, and was commercialised in the 1930s [3]. Recently, dehydrogenation has been used to produce propene for polypropylene manufacture and isobutene for methyl-*tert*-butyl ether (MTBE) synthesis [3], and the process accounts for about 3 [1] and 5% [2] of the total propene and butenes production, respectively. It has been estimated that the demand for propene will increase substantially in the future, about 5% annually [1], due to the growing use of polypropylene. Dehydrogenation is considered a viable option for increasing the supply of propene in areas such as the Middle East with cheap alkane feedstock available, and four new propane dehydrogenation projects are under development in this region [1, 4, 5]. MTBE production, on the other hand, will most likely decrease because of environmental reasons: MTBE has been found in the ground water due to leaking gasoline storage tanks. In parts of the United States its use as a fuel component has already been banned [6]. However, other uses for isobutene remain and technologies have been developed to convert the existing MTBE units to produce isooctane, another high quality fuel component [7, 8].

The dehydrogenation of alkanes, shown in general form in equation 1, is an endothermic equilibrium reaction. The reaction enthalpy for example in isobutane dehydrogenation is 122 kJ/mol at 550 °C [9].



At the moment, there are six industrial dehydrogenation processes, which are either in commercial operation or under development (Table 1).

**Table 1.** Industrial dehydrogenation processes [3, 10–16].

	<b>Catofin</b>	<b>UOP Oleflex</b>	<b>STAR<sup>a</sup></b>	<b>FBD<sup>b</sup></b>	<b>Linde</b>	<b>Statoil/Sintef</b>
<b>Licensor/developer</b>	Süd Chemie/ ABB Lummus	UOP Inc.	Uhde	Snamprogetti/ Yarsintez	Linde (BASF)	Statoil/ Sintef
<b>Reactor</b>	Adiabatic fixed-bed	Adiabatic moving bed	DH reactor + adiabatic oxyreactor	Fluidised bed	Isothermal fixed-bed	-
<b>Operation</b>	Cyclical	Continuous	Cyclical	Continuous	Cyclical	-
<b>Feed</b>	C <sub>3</sub> or C <sub>4</sub>	C <sub>3</sub> or C <sub>4</sub>	C <sub>3</sub> or C <sub>4</sub>	C <sub>3</sub> or C <sub>4</sub>	C <sub>3</sub> or C <sub>4</sub>	C <sub>3</sub>
<b>Catalyst</b>	CrO <sub>x</sub> /Al <sub>2</sub> O <sub>3</sub> with alkaline promoter	Pt/Sn/Al <sub>2</sub> O <sub>3</sub> with alkaline promoter	Pt/Sn on ZnAl <sub>2</sub> O <sub>4</sub> / CaAl <sub>2</sub> O <sub>4</sub>	CrO <sub>x</sub> /Al <sub>2</sub> O <sub>3</sub> with alkaline promoter	CrO <sub>x</sub> /Al <sub>2</sub> O <sub>3</sub>	Pt/hydro- talcite Mg(Al)O
<b>Heat import</b>	Heat formed in catalyst regeneration	Interstage heating	Heating of the DH reactor	Fuel added during regeneration	Heating of the reactors	-
<b>T (°C)</b>	590–650	550–620	DH: 550–590 ODH: <600	550–600	-	-
<b>p (bar)</b>	0.3–0.5	2–5	DH: 5–6 ODH: <6	1.1–1.5	>1	-
<b>Cycle time</b>	15–30 min	-	8 h	-	9 h	-
<b>Conversion (%)</b>	C <sub>3</sub> : 48–65 C <sub>4</sub> : 60–65	C <sub>3</sub> : 25 C <sub>4</sub> : 35	C <sub>3</sub> : 40	C <sub>3</sub> : 40 C <sub>4</sub> : 50	C <sub>3</sub> : 30	-
<b>Selectivity (%)</b>	C <sub>3</sub> : 82–87 C <sub>4</sub> : 93	C <sub>3</sub> : 89–91 C <sub>4</sub> : 91–93	C <sub>3</sub> : 89	C <sub>3</sub> : 89 C <sub>4</sub> : 91	C <sub>3</sub> : 90	-
<b>Note</b>	-	-	Combines DH+ODH	-	Pilot plant	Pilot plant

<sup>a</sup> Steam Active Reforming (STAR)

<sup>b</sup> Fluidised Bed Dehydrogenation (FBD)

DH = dehydrogenation, ODH = oxidative dehydrogenation

Most commercial dehydrogenation units use the Oleflex or the Catofin technology [4, 10]. All six processes include a dehydrogenation stage and a catalyst regeneration stage. Moreover, the STAR process includes an “oxydehydrogenation” stage [14]. The catalysts used in the processes are based on supported chromium oxide (chromia) or platinum metal. The thermodynamic limitations of dehydrogenation require efficient heat supply to the reaction; high temperatures close to 600 °C are needed for the process to proceed at an acceptable conversion level. Different approaches are applied to achieve this. For example in the STAR process the reactors are heated directly whereas the Catofin and the FBD processes utilise heat generated in the exothermal coke combustion taking place during catalyst regeneration.

## 1.2 Scope of the research

The chromia- and the platinum-based catalysts used in the industrial dehydrogenation processes have their own disadvantages. One problem related to supported chromia is that carcinogenic  $\text{Cr}^{6+}$  is formed during the regeneration stage. Platinum catalysts, on the other hand, are sensitive to impurities in the feed. Supported molybdenum and vanadium oxides have been studied as alternatives [17]. However, the currently used catalysts still remain superior and there is continuous interest for their further development.

The properties and dehydrogenation activity of supported chromia catalysts, mainly chromia on aluminium oxide (alumina), were investigated in this work. The aim was to obtain structure–activity data, which could be utilised in the optimisation of this catalytic system. The specific issues addressed in the research included the evaluation of chromium-based catalysts supported on different materials [I], the reduction and deactivation of chromia/alumina [II–V] and the mechanism of dehydrogenation [VI].

Transition aluminas are used extensively as catalyst supports due to several reasons. They are for example inexpensive and stable at relatively high temperatures [18]. However, alumina catalyses undesired side reactions, cracking and coke formation, which decrease selectivity and cause catalyst deactivation [19]. In industry, alumina-

supported catalysts are often promoted by alkali metals to neutralise the sites responsible for the unwanted reactions. In the present study, an aluminium nitride-modified alumina was tested as an alternative [I]. Platinum-based dehydrogenation catalysts have been found to benefit from a nitride-type support [20].

Reduction and deactivation are characteristic features of the supported chromia catalysts used in dehydrogenation. The reduction of chromia/alumina was investigated with different gases with the two aims of identifying the surface species formed during reduction and of evaluating their effect on the dehydrogenation behaviour of the catalyst [II–IV]. This was done by in situ infrared (IR) and Raman spectroscopic methods, which allowed the simultaneous measurement of the catalyst's surface characteristics and its activity.

Deactivation by coke formation or by structural changes necessitates frequent regeneration and ultimate replacement of the chromia/alumina catalyst in industrial processes. The in situ techniques were used to characterise the deactivating coke species formed during dehydrogenation [III, IV]. In addition, deactivation was compared for two chromia/alumina catalysts with different properties [V].

The aim in publication VI was to clarify the mechanism of alkane dehydrogenation on chromia/alumina catalysts. For this purpose several reaction mechanisms and kinetic models were evaluated. A mathematical model suitable for process simulation purposes was developed as a result.

## 2 SUPPORTED CHROMIA CATALYSTS

The structure and dehydrogenation behaviour of chromia catalysts have been studied extensively in an attempt to understand better how the properties of supported chromia affect the catalytic activity [21–32]. The system is complicated by the existence of chromium in several oxidation states and molecular structures [33]. These are influenced not only by the physical properties of the sample such as the support, the chromium loading and possible modifiers, but also by the conditions where the sample has been treated such as the calcination temperature. A short description is given below about the characteristics of oxidised and reduced chromia catalysts. Emphasis is given to the chromia/alumina system, which was investigated in this work. Other support materials that have been studied include silicon dioxide (silica) [28] and zirconium dioxide (zirconia) [34].

### 2.1 Oxidised chromia catalysts

Oxidised chromia catalysts contain  $\text{Cr}^{3+}$ ,  $\text{Cr}^{5+}$  and  $\text{Cr}^{6+}$  [22]. The relative amounts of these oxidation states depend mainly on the support material, the total chromium loading and the heat treatment. The dominant oxidation states on chromia/alumina catalysts are  $\text{Cr}^{3+}$  and  $\text{Cr}^{6+}$ ; only traces of  $\text{Cr}^{5+}$  have been detected by electron spin resonance (ESR) spectroscopy [19]. Figure 1 shows the correlation between the total chromium loading (in atoms of chromium per square nanometre of support) and the  $\text{Cr}^{3+}$  and  $\text{Cr}^{6+}$  loadings as determined for different chromia/alumina catalysts by wet-chemical methods [25–28]. The values were calculated from the data given in the respective reference and are trendsetting since the  $\text{Cr}^{6+}$  content depends on the catalyst calcination temperature [25] and the samples had been calcined at different temperatures (500 [27], 600 [25, 26] and 700 °C [28]). Two thirds of the possible  $\text{Cr}^{5+}$  in the catalyst is dissolved as  $\text{Cr}^{6+}$  in the wet-chemical determination [28].

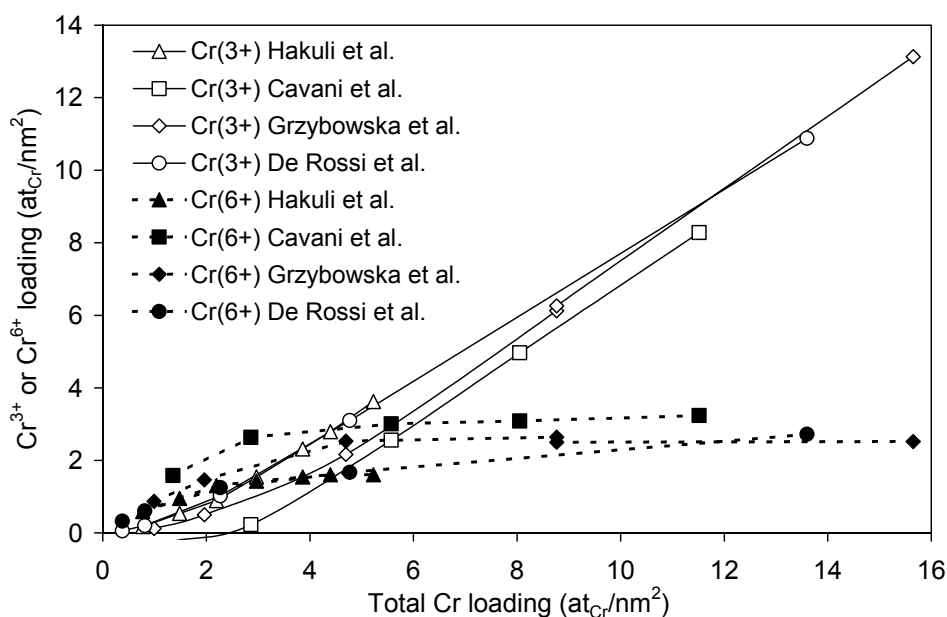


**Figure 1.** Correlation between the total chromium loading and the Cr<sup>3+</sup> and Cr<sup>6+</sup> loadings for different chromia/alumina catalysts as determined by Hakuli et al. [25], Cavani et al. [26], Grzybowska et al. [27] and De Rossi et al. [28].

At low chromium loading, mainly Cr<sup>6+</sup> is present on chromia/alumina. Two types of Cr<sup>6+</sup> have been detected by wet-chemical and spectroscopic methods [19, 22, 24–28]: (i) grafted Cr<sup>6+</sup>, which is in form of monochromates (CrO<sub>4</sub><sup>2-</sup>) and is insoluble in water and (ii) water-soluble Cr<sup>6+</sup> in form of polychromates (Cr<sub>2+x</sub>O<sub>7+3x</sub><sup>2-</sup>). The grafted Cr<sup>6+</sup> is chemically bonded to the support and its amount stabilises to about 0.8–1.1 at<sub>Cr(VI)</sub>/nm<sup>2</sup> (~1 wt-% chromium, depending on the support surface area) [24–28]. The total amount of Cr<sup>6+</sup> stabilises to about 2–3 at<sub>Cr(VI)</sub>/nm<sup>2</sup> (2–3 wt-%) for chromium loadings above 5 at<sub>Cr</sub>/nm<sup>2</sup> (4–8 wt-%) [24–28]. Increasing catalyst calcination temperature [25] decreases the amount of Cr<sup>6+</sup>.

Trivalent chromium is present at all chromium loadings and its amount increases with the total chromium content. The chromium(III) oxide phase is first dispersed on the support as an amorphous overlayer and then forms three-dimensional structures [24–28]. Monolayer coverage of chromia on alumina is defined as the coverage above which the three-dimensional chromia phase starts to grow but does not imply that the support surface would be totally covered. The monolayer limit has been determined to be about

4–5 at<sub>Cr</sub>/nm<sup>2</sup> with for example low energy ion spectroscopy (LEIS) [24] and Raman spectroscopy [29, 35]. X-ray diffraction (XRD) is less sensitive to small crystals and does not reveal crystalline  $\alpha$ -Cr<sub>2</sub>O<sub>3</sub> until above 8–10 at<sub>Cr</sub>/nm<sup>2</sup> (6–16 wt-%) [25–28].

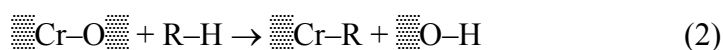
## 2.2 Reduced chromia catalysts

The dehydrogenation reactions take place in a reductive atmosphere where Cr<sup>6+</sup> and Cr<sup>5+</sup> present after oxidation are not stable but reduce to Cr<sup>3+</sup> and possibly to Cr<sup>2+</sup> [19, 21, 28]. Therefore, the involvement of Cr<sup>6+</sup> and Cr<sup>5+</sup> in dehydrogenation has been ruled out. The dehydrogenation activity of chromia catalysts is most often attributed to coordinatively unsaturated (c.u.s.) Cr<sup>3+</sup> ions [19, 21] although some authors have suggested that both Cr<sup>2+</sup> and Cr<sup>3+</sup> are active in dehydrogenation or that only Cr<sup>2+</sup> is active [36]. On reduced chromia/silica Cr<sup>2+</sup> has been detected for example by UV-Vis diffuse reflectance spectroscopy (DRS) [22]. On chromia/alumina its presence is not probable [19, 22] although temperature-programmed reduction (TPR) studies have suggested that the reduction may proceed below Cr<sup>3+</sup>, especially on catalysts with high chromium loading [37].

Varying with the sample properties and treatment conditions, several types of Cr<sup>3+</sup> exist on reduced catalysts [19, 21]: (i) redox Cr<sup>3+</sup> formed in the reduction of Cr<sup>6+</sup> and Cr<sup>5+</sup>, (ii) non-redox Cr<sup>3+</sup> in amorphous chromia phase, which is present both in reduced and oxidised samples and (iii) Cr<sup>3+</sup> present in crystalline chromia. In a broader sense redox Cr<sup>3+</sup> refers to chromium ions that have the potential to undergo reduction–oxidation cycles depending on the reaction environment. At low chromium loadings the redox and non-redox Cr<sup>3+</sup> sites can be in form of isolated ions but at high loadings they are located in clusters with other chromium ions. ESR spectroscopy reveals the presence of isolated ( $\delta$ -signal) and clustered Cr<sup>3+</sup> ( $\beta$ -signal) [22]. The dehydrogenation activity of chromia catalysts increases with the chromium loading [24–28] and the maximum activity of chromia/alumina has been reached with samples containing chromium about 8–9 at<sub>Cr</sub>/nm<sup>2</sup> [25, 26]. Above this the activity decreases most likely due to the formation of the XRD-detectable crystalline  $\alpha$ -Cr<sub>2</sub>O<sub>3</sub> [25, 26].

It is evident that both redox and non-redox  $\text{Cr}^{3+}$  are active in dehydrogenation [25, 26] and that crystalline  $\alpha\text{-Cr}_2\text{O}_3$  is the least active of the  $\text{Cr}^{3+}$  phases [26]. Otherwise it remains undecided whether the origin and the environment of the  $\text{Cr}^{3+}$  affect its activity. Hakuli et al. [25] and De Rossi et al. [28] proposed that the redox  $\text{Cr}^{3+}$  ions are the active sites at low chromium loadings, and at high loadings both redox and non-redox sites are active. On the other hand, Cavani et al. [26] suggested that non-redox  $\text{Cr}^{3+}$  in the amorphous chromia phase is more active than  $\text{Cr}^{3+}$  formed by reduction. Both mononuclear (isolated) [28] and multinuclear (clustered) [31] chromium ions have been indicated as the most active sites. However, it has also been concluded that the size of the  $\text{Cr}^{3+}$  oxide cluster does not affect the activity of the  $\text{Cr}^{3+}$  ions in dehydrogenation [25] or in octane aromatisation [38].

In addition to the  $\text{Cr}^{3+}$  ions, the surface oxygen ions have been proposed to be involved in the dehydrogenation reaction [19, 39–41]. The dehydrogenation may proceed via dissociation of the alkane molecule to an alkyl group bonded to surface chromium and a hydrogen atom bonded to surface oxygen, as shown in equation 2.



In the equation, symbol  $\begin{array}{c} \square\square\square \\ \square\square\square \\ \square\square\square \end{array}$  denotes the surface. In this case the active site would be a pair of c.u.s. chromium and oxygen ions regardless of the quality of the  $\text{Cr}^{3+}$ .

### 3 EXPERIMENTAL

The experimental procedures are described in detail in publications I–VI and only a short summary is given here.

#### 3.1 Preparation and characterisation of catalysts

Most of the catalysts investigated in this study were prepared by the atomic layer deposition (ALD) method with chromium(III) acetylacetonate ( $\text{Cr}(\text{acac})_3$ ;  $\text{Cr}(\text{C}_5\text{O}_2\text{H}_7)_3$ ) as the chromium precursor [I–V]. In addition, two alumina-supported chromia catalysts developed for fluidised-bed operation, FB1 [V] and FB2 [VI], were used. Because the FB samples were obtained from a commercial source the details of their preparation are unknown.

The ALD method, or earlier known as the atomic layer epitaxy (ALE) method, relies on separate, saturating reactions of gaseous precursor compounds on solid materials [42]. Chromia/alumina catalysts active in the dehydrogenation of light alkanes have been prepared earlier by this technique by Kytökivi et al. [24] and Hakuli et al. [25]. The ALD preparation of chromia catalysts consists of three steps [21, 42]: (i) pretreatment of the support, (ii) chemisorption of gaseous  $\text{Cr}(\text{acac})_3$  on the solid support at 200 °C and (iii) removal of the acac ligands at elevated temperature. The amount of chromium in the catalyst can be increased by repeating in cycles steps (ii) and (iii). Three sets of ALD-prepared samples were used in this study. Information about the preparation and the properties of the catalysts can be found below and in Table 2.

**Set 1:** Samples prepared on Akzo Nobel 000-1.5E  $\gamma$ -alumina by use of air as the ligand removal agent (alumina particle size specified in Table 2, calcined in air at 600 °C for 16 h, final catalyst calcination in air at 600 °C for 4 h) [II–V]. These are referred to in the text as  $X\text{Cr}/\text{Al}$ , with  $X$  indicating the chromium content of the sample.

**Set 2:** Samples prepared on Akzo Nobel 001-1.5E  $\gamma$ -alumina by use of air, water or ammonia as the ligand removal agent (alumina particle size 0.25–0.50 mm, calcined in

air at 800 °C for 16 h and in vacuum at 560 °C for 3 h) [I]. These are referred to in the text as Cr/Al-*Y*, with *Y* indicating the ligand removal agent.

**Set 3:** Samples prepared on aluminium nitride-modified Akzo Nobel 001-1.5E  $\gamma$ -alumina by use of ammonia as the ligand removal agent [I]. The modification of the alumina support (pretreated as in Set 2) is described in publication I and in detail by Puurunen [42]. In short, it consisted of repeating in cycles the separate reactions of gaseous trimethylaluminium (TMA) and ammonia on the bare  $\gamma$ -alumina support to yield AlN/Al<sub>2</sub>O<sub>3</sub>-type materials containing different amounts of nitrogen. The samples are denoted as Cr/*n*-AlN-NH<sub>3</sub>, with *n* indicating the number of TMA and ammonia cycles, and NH<sub>3</sub> the acac ligand removal agent.

Pure chromia ( $\alpha$ -Cr<sub>2</sub>O<sub>3</sub>, Aldrich, 98+) and the alumina supports were used as reference materials.

**Table 2.** Information about the samples used in the study.

Sample	Content (wt-%)		Support	Preparation	Ref.
	Cr	Cr <sup>6+</sup>			
1.2Cr/Al	1.2	0.9	Akzo 000, 0.2–0.4 mm	1 cycle of Cr(acac) <sub>3</sub> and air	[IV]
7.5Cr/Al	7.5	2.9	Akzo 000, 0.7–1.0 mm	6 cycles of Cr(acac) <sub>3</sub> and air	[IV]
13.5Cr/Al	13.5	3.0	Akzo 000, 0.25–0.50 mm	12 cycles of Cr(acac) <sub>3</sub> and air	[II–V]
Cr/Al-O <sub>2</sub>	1.0	<i>n.a.</i>	Akzo 001	1 cycle of Cr(acac) <sub>3</sub> and air	[I]
Cr/Al-H <sub>2</sub> O	1.0	<i>n.a.</i>	Akzo 001	1 cycle of Cr(acac) <sub>3</sub> and H <sub>2</sub> O	[I]
Cr/Al-NH <sub>3</sub>	1.1	<i>n.a.</i>	Akzo 001	1 cycle of Cr(acac) <sub>3</sub> and NH <sub>3</sub>	[I]
Cr/2·AlN-NH <sub>3</sub>	1.1	<i>n.a.</i>	AlN-modified Akzo 001	Support: 2 cycles of TMA and NH <sub>3</sub> , Catalyst: 1 cycle of Cr(acac) <sub>3</sub> and NH <sub>3</sub>	[I]
Cr/6·AlN-NH <sub>3</sub>	1.1	<i>n.a.</i>	AlN-modified Akzo 001	Support: 6 cycles of TMA and NH <sub>3</sub> , Catalyst: 1 cycle of Cr(acac) <sub>3</sub> and NH <sub>3</sub>	[I]
FB1	12	1.0	Alumina	Unknown	[V]
FB2	12	1.3	Alumina	Unknown, catalyst contained a modifying component	[VI]
Chromia	-	0.1	-	-	[II–IV]

*n.a.* not analysed

The chromium contents of the catalysts were measured by atomic absorption spectroscopy (AAS) or by instrumental neutron activation analysis (INAA). The carbon contents of some samples were determined either by Ströhlein CS-5500 analyser or by LECO CHN-600 analyser, which was also used for nitrogen content analyses. Surface area measurements were done by the Brunauer–Emmett–Teller method (BET) and crystalline species were detected by XRD spectroscopy.

Cr<sup>6+</sup> contents were measured by UV-Vis spectrophotometry after dissolution of the Cr<sup>6+</sup> in a basic aqueous solution as described elsewhere [43]. In the determination, Cr<sup>5+</sup> possibly present in the catalyst is partly dissolved with the Cr<sup>6+</sup> [28]. Chromium oxidation states were probed by X-ray photoelectron spectroscopy (XPS) and ESR spectroscopy. The local atomic structure of chromium was studied by X-ray absorption spectroscopy (XAS). Ex situ diffuse reflectance Fourier transform infrared (DRIFT) spectra were recorded for some samples to investigate the type of species formed in the chemisorption of Cr(acac)<sub>3</sub>. Temperature-programmed reduction with hydrogen (H<sub>2</sub>-TPR) was used to study the reduction of the catalysts.

### 3.2 In situ spectroscopic measurements

The reduction of the catalysts and the formation of adsorbed surface species during reduction and dehydrogenation were investigated by in situ DRIFTS [II–IV] and by in situ Raman spectroscopy [II, III]. Experiments were done as a function of temperature from 25 to 580 °C, and as a function of time on stream at 580 °C as described in the publications.

The in situ DRIFTS measurements were performed with a Nicolet Nexus Fourier transform infrared (FTIR) spectrometer equipped with a Spectra-Tech reaction chamber. Gaseous products were monitored by an Omnistar mass spectrometer (MS). Measurements were done with hydrogen [II–IV], carbon monoxide [II, IV], propane [III], isobutane [IV] and isobutene [IV]. In hydrocarbon experiments the reaction chamber was flushed with inert gas periodically. Gaseous hydrocarbons have strong IR bands at 3100–2800 cm<sup>-1</sup> and their removal was necessary for the detection of adsorbed species on the samples.

The in situ Raman spectrometric measurements were done with a Renishaw Micro-Raman System-1000 equipped either with a Linkam TS-1500 in situ sample treatment chamber [II] or with a homemade fixed bed reactor [III] described in detail by Guerrero-Pérez et al. [44]. Gaseous products were analysed by a Varian 3800 gas chromatograph (GC) equipped with a thermal conductivity detector. Measurements were done with

hydrogen [II, III], carbon monoxide (unpublished) and propane [III]. To enable comparison with the DRIFTS results, the samples were flushed periodically with inert gas during the experiments with propane.

### **3.3 Dehydrogenation activity measurements**

The dehydrogenation activity measurements were done in a fixed bed microreactor system equipped with a Gaset FTIR gas analyser (Temet Instruments Ltd.) and an HP 6890 GC for product analysis.

The activities of the catalysts were studied in cycles of (pre)reduction–dehydrogenation–regeneration. The reduction of the catalyst was accomplished either with hydrogen or carbon monoxide before the dehydrogenation, or with alkane during the first minutes on alkane stream. Isobutane dehydrogenation activities were measured under atmospheric pressure at 520–580 °C [I, IV–VI]. After the dehydrogenation, the samples were regenerated with diluted air.

The reduction products (carbon monoxide, carbon dioxide and water) were measured by FTIR, the dehydrogenation products by FTIR and GC, and the regeneration products (carbon monoxide, carbon dioxide and water) by FTIR. The amount of coke deposited on the catalyst during dehydrogenation was calculated from the amounts of carbon oxides measured during regeneration. Further details of the FTIR gas analysis method and of the determination of the product distribution based on the measured spectra can be found elsewhere [VI, 45]. The conversions, selectivities and yields were calculated on molar basis as described in publication VI.

### **3.4 Kinetic modelling of isobutane dehydrogenation**

In the kinetic modelling study [VI], different reaction rate equations were derived on the basis of four dehydrogenation mechanisms, assuming either adsorption of isobutane or abstraction of hydrogen from the adsorbed species as the rate-determining step. The modelling was done based on isobutane dehydrogenation activity measurements

performed for the FB2 catalyst at 520–580 °C under atmospheric pressure. The parameters of the derived equations were estimated by the Kinfit program [46] by minimising the sum of squares of the residuals (SSR) between the measured and calculated compositions of the product stream.

## 4 RESULTS AND DISCUSSION

### 4.1 Chromium catalysts supported on aluminium nitride-modified alumina

The effect of modifying the alumina support with a basic material was studied for chromium catalysts prepared on aluminium nitride-modified alumina [1]. The aim was to increase the activity and selectivity in dehydrogenation compared to chromia supported on alumina.

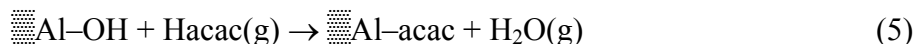
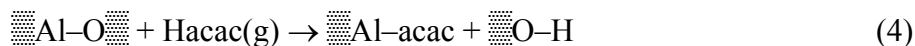
The industrial chromia/alumina catalysts are generally promoted with alkali metals [11]. The promoters have been suggested to affect the catalysts by two ways: by increasing the number of active sites [26] and by decreasing the acidity of the alumina support which causes cracking and coke formation [11, 19]. The use of a basic aluminium nitride-type support might also be beneficial. If the active site in dehydrogenation is a cation–anion pair, the replacement of the oxygen ions with more basic nitrogen could increase the dehydrogenation activity of the site. Furthermore, the basic aluminium nitride might decrease the acidity of the alumina support. It has been found that mesoporous vanadium nitrides are active in the dehydrogenation of *n*-alkane with high selectivity to *n*-alkenes [47], and the dehydrogenation activity of Pt/AlPO(N) catalysts increases with the nitrogen content and, thus, basicity of the support [20].

#### 4.1.1 Chemisorption of $\text{Cr}(\text{acac})_3$

Chromium catalysts have earlier been prepared by the ALD method on oxide supports [24, 25]. In this work, the chemisorption of  $\text{Cr}(\text{acac})_3$  on unmodified aluminas pretreated at 200–800 °C and on the aluminium nitride-modified supports was compared. Samples with acac ligands intact were investigated for this purpose.

When  $\text{Cr}(\text{acac})_3$  chemisorbs on alumina, it binds to surface OH groups and c.u.s. Al–O sites [24, 25]. In the present study a combination of a ligand exchange reaction with surface OH groups (equation 3) [24, 25] and readsorption of the released Hacac (equation 4 and/or 5) [48] seemed to take place during the chemisorption of  $\text{Cr}(\text{acac})_3$

on the unmodified alumina supports. Dissociative adsorption of Cr(acac)<sub>3</sub> on alumina Al–O pairs (equation 6) [25] may have occurred, too.



Similar reactions can probably take place with Al–NH<sub>x</sub> sites and c.u.s. Al–N sites on the AlN/Al<sub>2</sub>O<sub>3</sub> supports.

The acac ligand density on the surface settled at a more or less constant value (about 1.9 acac/nm<sup>2</sup>) in the chemisorption of Cr(acac)<sub>3</sub> on the unmodified and modified aluminas. The factor determining the surface saturation of the chemisorbed Cr(acac)<sub>3</sub> can be a shortage of suitable bonding sites, for example OH groups, or steric hindrance imposed by the acac ligands. Because the acac ligand density did not depend on the OH group content of the supports, it was concluded that the steric hindrance by the acac ligands determined the saturation not only on alumina [24, 25] but also on the aluminium nitride-modified aluminas.

#### 4.1.2 Activity in dehydrogenation

The effect of the aluminium nitride modification on the dehydrogenation behaviour was evaluated after acac ligand removal for the Cr/2·AlN-NH<sub>3</sub> and Cr/6·AlN-NH<sub>3</sub> catalysts with 0.8 and 3.1 wt-% nitrogen, respectively. Due to the easy oxidation and hydrolysis of the aluminium nitride material, ammonia was used for the ligand removal. Because chromium catalysts have generally been prepared by use of air [24, 25], catalysts prepared on unmodified alumina by use of ammonia, water and air were compared. Ammonia was not as efficient as air or water in removing the acac ligands but left behind some carbon residue in an amount that increased with the nitrogen content of the sample. All catalysts contained chromium about 1 wt-% (Table 2).

The activities of the Cr/Al-*Y* and Cr/*n*-AlN-NH<sub>3</sub> catalysts were measured in the dehydrogenation of isobutane at 580 °C under atmospheric pressure, without any prereduction. The highest activity was obtained with the catalyst prepared on unmodified alumina by use of air for ligand removal (Figure 2). No clear differences were observed between the selectivities of the samples. The Cr/Al-O<sub>2</sub> catalyst was the only one that contained any significant amounts of reduced chromium species in the first dehydrogenation stage. In the second stage, after the oxidative regeneration, all five samples contained Cr<sup>3+</sup> formed by reduction in addition to non-redox Cr<sup>3+</sup>.

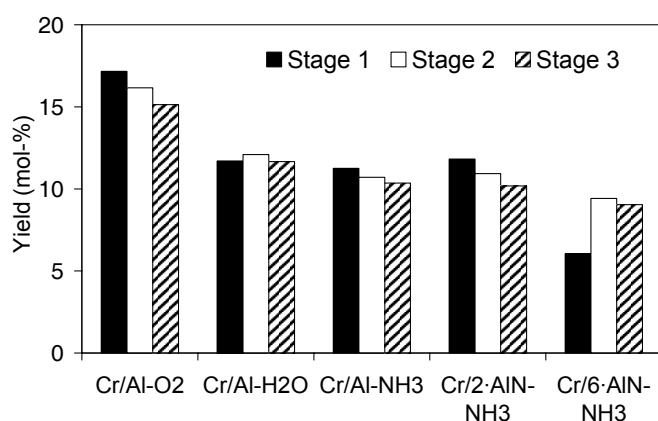


**Figure 2.** Yield of isobutene at 10 min on isobutane stream with the Cr/Al-*Y* and Cr/*n*-AlN-NH<sub>3</sub> catalysts as measured by GC at 580 °C, 1.03 bar, WHSV=15 h<sup>-1</sup> and nitrogen dilution 3 mol/7 mol. [I]

Aluminium nitride modification of the alumina support increased neither the conversion of isobutane nor the selectivity to isobutene contrary to what was sought for. However, the main side reaction, cracking of isobutane was mainly a thermal reaction and therefore it was not possible to observe significant differences between the selectivities of the samples. The decrease in activity with increasing nitrogen content of the catalyst could not be explained by the residual carbon left behind in the ligand removal with ammonia. Instead, it appeared that the presence of nitrogen on the surface was not beneficial. If the active site is a cation–anion pair, as has been proposed [39–41], it seems that Cr–N pairs are not as active as Cr–O pairs in the dehydrogenation of isobutane. The activity increase observed in the second cycle for the Cr/6-AlN-NH<sub>3</sub> catalyst after oxidative regeneration, which destroyed the nitride phase at least partly, supports this proposal.

For the catalysts prepared on unmodified alumina, ligand removal with water or ammonia decreased the dehydrogenation activity. Water removed the acac ligands as efficiently as air. Therefore, the decrease in activity was probably not due to residual carbon from any unremoved acac ligands. Instead, it was most likely caused by a lower number of exposed chromium sites present on the water- or ammonia-treated catalysts: the Cr/Al-O<sub>2</sub> sample had higher surface area than the water-treated one, and higher surface Cr/Al ratio (unpublished XPS results) than either the water- or the ammonia-treated sample, both results suggesting that water and ammonia had sintered the catalyst more than air. Furthermore, the fresh Cr/Al-O<sub>2</sub> catalyst contained the highest amount of Cr<sup>6+</sup> before the first dehydrogenation stage, which may have contributed to its activity. Cr<sup>6+</sup> is more mobile than Cr<sup>3+</sup> [49] and it is possible that more multinuclear (clustered) chromium species, which have been proposed to be more active than isolated Cr<sup>3+</sup> ions [31, 34], were formed on this catalyst.

It is notable that all the samples were active in the first dehydrogenation stage irrespective of whether they contained Cr<sup>3+</sup> formed by reduction. Furthermore, the activities of the Cr/Al-H<sub>2</sub>O, Cr/Al-NH<sub>3</sub> and Cr/2·AlN-NH<sub>3</sub> catalysts did not increase markedly after the first regeneration, which oxidised some of the chromium. Therefore, the activity of Cr<sup>3+</sup> seems to be determined mainly by its structural environment and not by whether it has been formed through reduction. Earlier, it has been proposed that the redox sites are the only active sites at low chromium loadings [24, 25, 28]. It is probable though that non-redox Cr<sup>3+</sup> sites are also active in accordance with Cavani et al. [26] who suggested that Cr<sup>3+</sup> ions in the amorphous chromia phase are more active than the redox Cr<sup>3+</sup> sites.

## 4.2 Reduction of chromia/alumina

The reduction of chromia/alumina was studied to identify the surface species formed during reduction and to clarify the significance of these species to the behaviour of the catalyst during dehydrogenation. When oxidised chromia/alumina catalysts are contacted with alkane, the reduction of Cr<sup>6+</sup> (and Cr<sup>5+</sup>) results in release of carbon oxides and water. Thereafter, dehydrogenation products start to form. The initial

combustion period can be avoided if the catalyst is prereduced before the dehydrogenation stage with for example hydrogen, carbon monoxide or methane; prereduction is used for example in the Catofin process [3].

However, in some cases prereduction with hydrogen or carbon monoxide results in a lower activity in dehydrogenation compared to reduction with the alkane feed [17, 21, 23, 32]. Furthermore, carbon monoxide may increase side reactions—cracking and coke formation—during dehydrogenation [21, 23]. These effects may be related to the surface species formed during reduction [21]: indirect measurements have indicated that reduction by hydrogen and alkanes leads to retainment of water on the catalyst, and reduction by carbon monoxide to deposition of carbonaceous material [17, 21].

#### **4.2.1 Reduction measurements**

The reduction of chromia/alumina by hydrogen, carbon monoxide, propane and isobutane was investigated in detail for the 13.5Cr/Al catalyst by ex situ and in situ spectroscopic methods [II–IV, 50]. This sample was chosen for closer examination primarily for two reasons: (i) the chromium content of the sample ( $8.0 \text{ at}_{\text{Cr}}/\text{nm}^2_{\text{support}}$ ;  $9.4 \text{ at}_{\text{Cr}}/\text{nm}^2_{\text{sample}}$ ) coincided with the range where the highest activity in dehydrogenation has been observed, 8–9  $\text{at}_{\text{Cr}}/\text{nm}^2$  [25, 26] and (ii) the catalyst had been prepared by the ALD method, which produces well-dispersed surface species [24, 25]. Additional measurements were done for the pure chromia and alumina samples [II–IV] and for the 1.2Cr/Al (unpublished results, IV) and 7.5Cr/Al catalysts [IV]. The reduction behaviour of the 13.5Cr/Al and FB1 catalysts [V] is compared in a later section.

#### **4.2.2 Structural changes during reduction**

The structure of the 13.5Cr/Al catalyst after calcination and reduction [II–IV] corresponded to that generally reported for chromia/alumina catalysts with high chromium loading [19, 21, 26]. After calcination, chromium was present mainly as octahedrally coordinated  $\text{Cr}^{3+}$  and tetrahedrally coordinated  $\text{Cr}^{6+}$ , which were in form of amorphous  $\text{Cr}^{3+}$  oxide and polymeric chromates, respectively. Crystalline  $\text{Cr}_2\text{O}_3$  was not

found by XRD or Raman spectroscopy indicating that the ALD method was able to produce well-dispersed chromia species even at this level of loading.

The reduced chromium oxidation state was probed spectroscopically by XPS and XAS [II], and indirectly by FTIR gas analysis of the gaseous products released in reduction at 580 °C [IV]. The oxidation state of chromium appeared to be the same, about +3, after reduction by hydrogen, carbon monoxide or alkane, which agrees with findings by others [17, 19, 21]. The  $\text{Cr}^{3+}$  was in octahedral configuration at least after hydrogen reduction [II]. No clear evidence for  $\text{Cr}^{2+}$  was found, but its presence was not ruled out completely.  $\text{Cr}^{2+}$  has generally not been detected on chromia/alumina [19], although it has been speculated [37] that, at high chromium loadings, chromium reducible to  $\text{Cr}^{2+}$  could exist as supported on microcrystalline or amorphous chromia and, therefore, without direct contact with the alumina support. The formation of  $\text{Cr}^{2+}$  has been observed on crystalline chromia [51] and on chromia/silica [39, 52], which contains crystalline chromia species even at low chromium loadings [21].

Clustering of the chromia phase has been suggested to take place during reduction of chromia/alumina [21] and chromia/zirconia [38]. Some indication that clustering may have happened on the 13.5Cr/Al catalyst was found by Raman spectroscopy, XPS and DRIFTS [II, III]. Raman spectroscopic measurements suggested formation of more crystalline chromia during reduction by hydrogen [II] and carbon monoxide (unpublished results). Moreover, XPS measurements indicated a decrease in the Cr/Al ratio and DRIFTS measurements the formation of Al–OH species with reduction, both results suggesting that more alumina surface was exposed. Thus, the well-dispersed chromia phase obtained by the ALD technique was not stable under the reduction conditions.

#### ***4.2.3 Surface species formed during reduction***

The formation of hydroxyl groups and carbon-containing species during reduction was investigated by in situ DRIFT and Raman spectroscopies at 580 °C and as a function of temperature from 25 to 580 °C [II–IV, 50]. Figure 3 shows DRIFT spectra measured for

the 13.5Cr/Al catalyst after calcination and after reduction at 580 °C. The chromate band disappeared within the first minutes on gas stream, indicating that the catalyst was reduced in the in situ chamber. Hydroxyl species were formed from hydrogen and the alkanes, and carbon-containing species from carbon monoxide and the alkanes. The 1.2Cr/Al catalyst showed similar behaviour (unpublished results, IV).

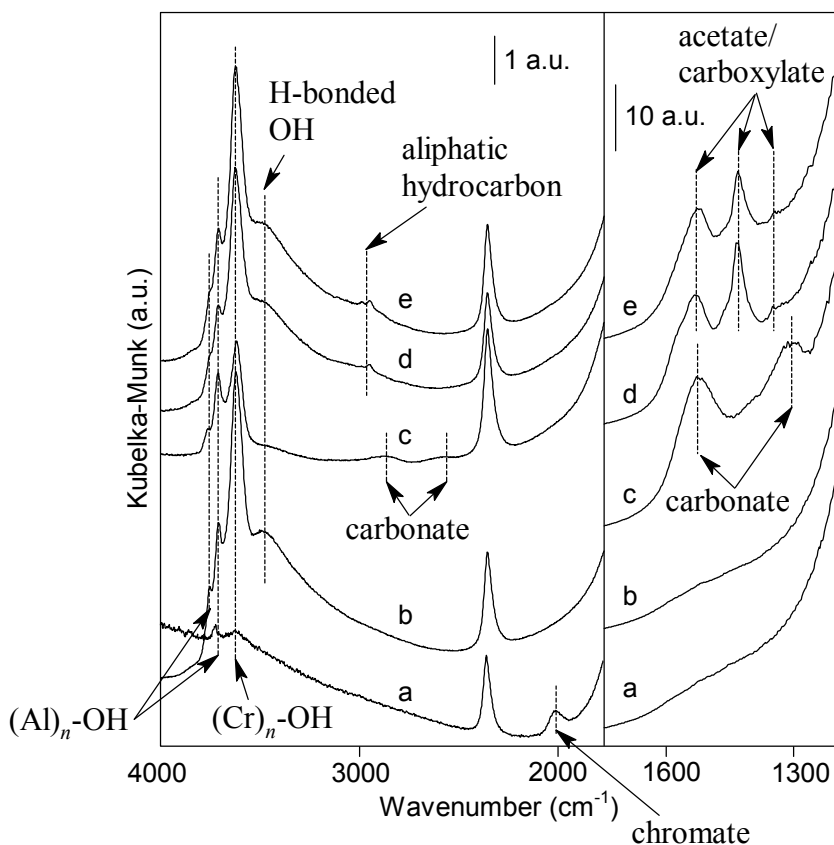


**Figure 3.** DRIFT spectra measured for the 13.5Cr/Al catalyst after (a) calcination, and reduction by (b) H<sub>2</sub>, (c) CO, (d) propane and (e) isobutane at 580 °C. Spectra were measured under inert gas after a 15 min reduction (b and c) or after 3 min on alkane stream (d and e).

The reduction of chromia/alumina by hydrogen released gaseous water. For the 13.5Cr/Al catalyst, the amount of water detected by FTIR gas analysis at 580 °C was lower than the amount calculated assuming reduction of Cr<sup>6+</sup> to Cr<sup>3+</sup> [IV]. It has been estimated that about 30–50% [17, 23, 39, 53] of the total amount of water produced remains on the reduced surface. This water was present as isolated hydroxyl groups bonded to the chromia and alumina phases and as associated hydrogen-bonded

hydroxyls, shown schematically in Figure 4 with their IR band positions at ~200–580 °C. The isolated hydroxyl species were most likely terminal and bridging on both chromia [54] and on alumina [55, 56]. The  $(\text{Cr})_n\text{-OH}$  bands were observed as one peak at high temperatures due to thermal effects.  $(\text{Cr})_n\text{-OH}$  species at similar wavenumbers formed on bulk chromia. The formation of  $(\text{Cr})_n\text{-OH}$  species on chromia/alumina indicated that some of the c.u.s. chromium ions formed in the reduction were saturated by hydroxyl groups. This most likely decreased the potential activity of the catalyst in dehydrogenation. No Cr–H species, which should appear at 1714 and 1697  $\text{cm}^{-1}$  [57], were detected but their presence is not ruled out.

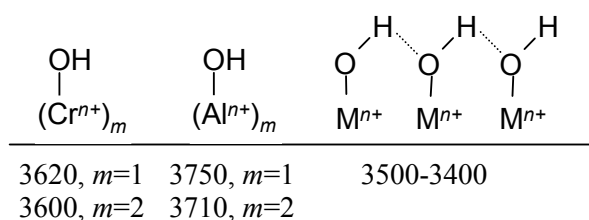


**Figure 4.** Hydroxyl species formed on chromia/alumina during hydrogen reduction [II]. Approximate structures based on [54, 58]. Band positions are in units of  $\text{cm}^{-1}$  and depended on the measurement temperature; values at room temperature were ca. 20  $\text{cm}^{-1}$  higher than those given in the figure.  $n=3$ ,  $M=\text{Al}$  or  $\text{Cr}$ .

Reduction of chromia/alumina at 580 °C by carbon monoxide resulted in formation of gaseous carbon dioxide and surface carbonates, which were most likely monodentate [IV]. Bicarbonates, adsorbed carbon monoxide, formates, carbonates and possibly inorganic carboxylates (Figure 5) were detected during temperature-programmed DRIFTS measurements with carbon monoxide [II]. Bulk chromia showed similar behaviour. The peaks due to monodentate carbonates at about 1530 and 1310  $\text{cm}^{-1}$  were attributed to formates in publication II because carbonates and formates have overlapping bands in this region. The presence of formates bonded to chromia and alumina was evident, though, from their characteristic bands at the C–H region.

adsorbed CO	bicarbonate	formate on chromia	formate on alumina	monodentate carbonate	bidentate carbonate	inorganic carboxylate
~2200	1620 1430 1220	2960, 2880 1560, 1380 1350	3009, 2930 (1590, 1390)	2870 2580 1530 1310	*	*

**Figure 5.** Carbon-containing species formed on chromia/alumina during carbon monoxide reduction [II, IV]. Approximate structures based on [59, 60]. Wavenumber values are in units of  $\text{cm}^{-1}$ . \*Species possibly present.  $n=3$  (and possibly 2).

Reduction of chromia/silica by carbon monoxide has been proposed to occur through formation of intermediate bicarbonate species, which is transformed into carboxylate (formate) in the reduction [61]. Reduction of  $\text{Cr}^{6+}$  on oxidised chromia, on the other hand, has been suggested to occur during the formation of the bicarbonate and carbonate species [62]. The present results supported the involvement of bicarbonates in the reduction. Further reactions of the bicarbonates probably resulted in the formates, carboxylates and carbonates. In addition, bicarbonates may have formed in reaction between the chromia surface and carbon dioxide released in the reduction, and formates in reaction of surface hydroxyls with gaseous/adsorbed carbon monoxide [62]. Adsorbed carbon monoxide indicated the presence of c.u.s.  $\text{Cr}^{3+}$  (and possibly  $\text{Cr}^{2+}$ ). Bands due to hydroxyl species increased during the reduction. Since water cannot form from carbon monoxide, the hydroxyls were present already on the calcined surface or formed from feed impurities. Therefore, their amount was most likely very low.

Interaction of propane and isobutane with calcined chromia/alumina and bulk chromia released gaseous carbon oxides and resulted in formation of surface acetone, formates, acetates/carboxylates and hydroxyls in temperature-programmed DRIFTS measurements with propane and isobutane [III, IV, 50]. Comparison of the results with literature [63] suggested that the reactions presented in Figure 6 took place on the samples, with  $\text{Cr}^{6+}$  reducing simultaneously with the formation of the alkoxide groups. At higher temperatures where dehydrogenation of alkanes took place aliphatic and unsaturated/aromatic hydrocarbon species were detected by DRIFTS and Raman

spectroscopy [III, IV] and graphite-like deposits by Raman spectroscopy [III], but these were most likely formed as a result of dehydrogenation.

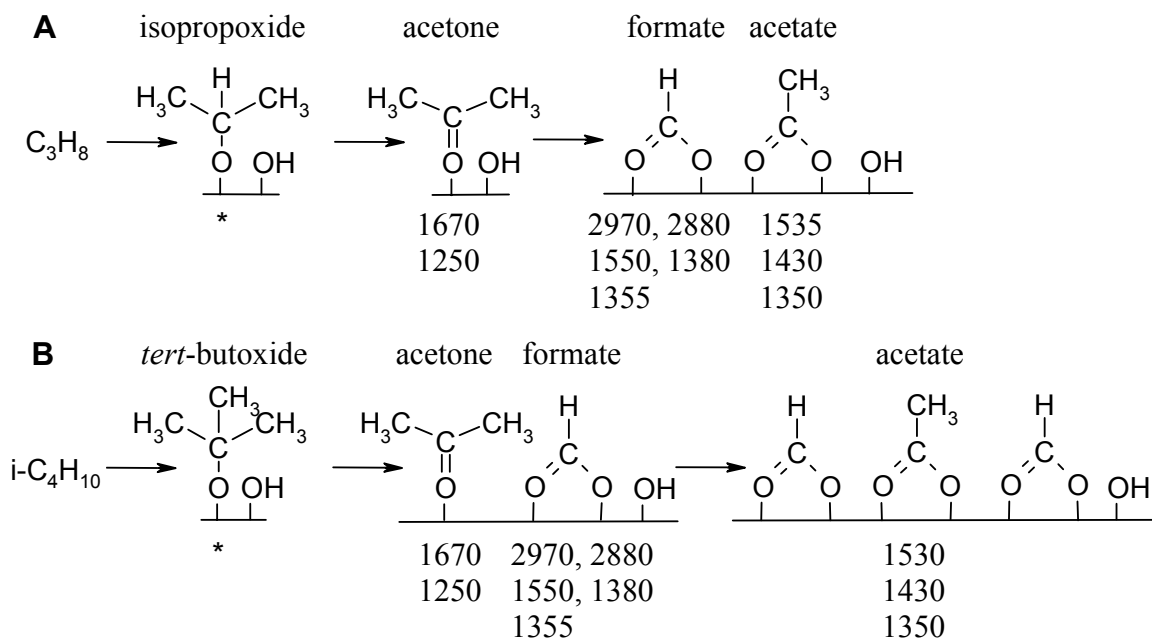


**Figure 6.** Formation of oxygen-containing carbon species during reduction of chromia/alumina with (A) propane and (B) isobutane [III, IV, 50]. Approximate structures based on [63]. Wavenumber values are in units of  $cm^{-1}$ . The scheme does not reflect the real stoichiometries of the reactions. \*The species was not detected but was assumed to form in accordance with [63].

Some of the water formed in the reduction with alkanes was retained on the catalysts and was present as hydroxyl species [IV]. The hydroxyl peaks were observed at similar wavenumbers as after hydrogen reduction. Thus, similar alumina- and chromia-bonded hydroxyls and hydrogen-bonded hydroxyls were formed as shown in Figure 4 [III, IV].

Some similarities and differences between the surfaces reduced by hydrogen, carbon monoxide and the alkanes were concluded from the DRIFTS results [IV]. Similar hydroxyl species formed from hydrogen and the alkanes. The carbon monoxide-reduced surface contained the lowest number of hydroxyl groups, and therefore most likely the highest number of c.u.s. sites able to participate in hydrocarbon reactions. On the other hand, the carbon monoxide- and the alkane-reduced surfaces contained carbonaceous deposits, which may have covered part of the active chromia phase.

### 4.3 Calcined and prereduced chromia/alumina in dehydrogenation

#### 4.3.1 Activity in dehydrogenation

The effect of the species formed during reduction on the behaviour of chromia/alumina in alkane dehydrogenation was investigated by activity measurements [IV] and by in situ spectroscopic techniques at 580 °C [III, IV, 50]. Another aim was to identify carbon-containing species formed during dehydrogenation, which cause deactivation. Figure 7 shows the activity of the 13.5Cr/Al catalyst in dehydrogenation of isobutane at 580 °C after calcination, and after prereduction by hydrogen or carbon monoxide.

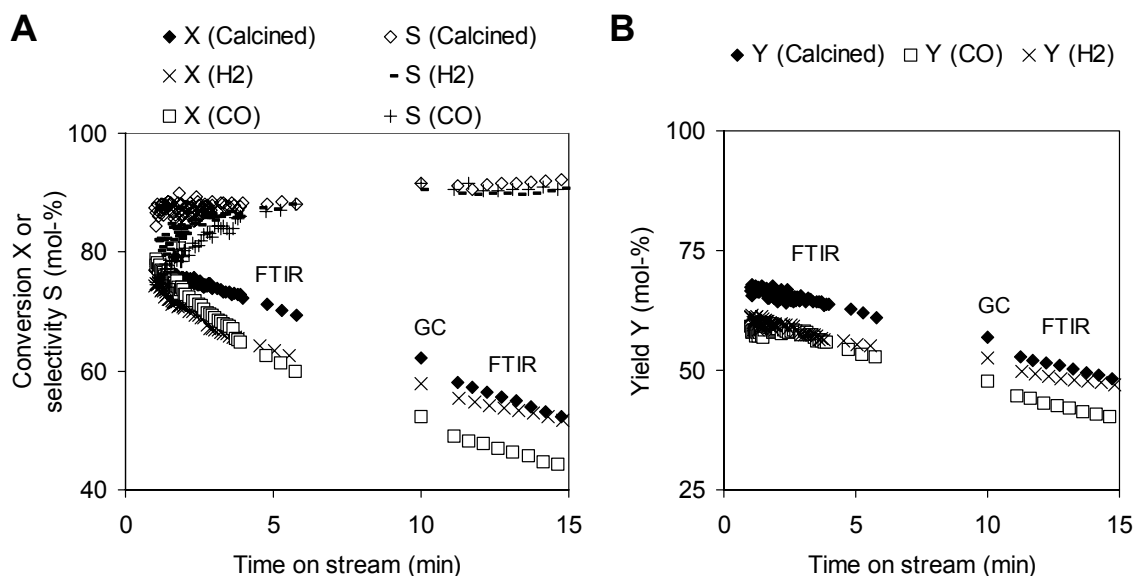


**Figure 7.** (A) The conversion of isobutane (X) and selectivity to isobutene (S), and (B) the yield of isobutene (Y) for the 13.5Cr/Al catalyst after calcination and after H<sub>2</sub> or CO prereduction at 580 °C, 1.03 bar, WHSV=5 h<sup>-1</sup> and nitrogen dilution 1 mol/9 mol. [IV]

The highest initial conversion of isobutane was obtained with the carbon monoxide-prereduced surface. However, the yield of isobutene was decreased by high initial cracking activity to C<sub>1</sub>–C<sub>3</sub> hydrocarbons. Hydrogen prereduction decreased the activity in dehydrogenation, too. Thus, the highest yield of isobutene was obtained after calcination, in agreement with other studies [17, 21]. The dehydrogenation activity decreased rapidly with time on stream with increase in selectivity although hydrogen

prereduction seemed to inhibit the deactivation slightly. The coke contents of the calcined, hydrogen- and carbon monoxide-prereduced catalysts after the 15 min dehydrogenation were 2.9, 2.3 and 3.6 mmol/g<sub>cat</sub>, respectively. The amount of coke on the catalyst increased fairly linearly with time on stream with a decrease in the H/C ratio [IV].

#### **4.3.2 Surface species formed during dehydrogenation**

The surface species formed during propane and isobutane dehydrogenation were investigated by in situ spectroscopic methods. Propane dehydrogenation was followed after calcination and hydrogen prereduction for the 13.5Cr/Al catalyst by DRIFT and Raman spectroscopies [III], and isobutane dehydrogenation for the calcined and hydrogen- or carbon monoxide-prereduced 1.2Cr/Al (unpublished results) and 13.5Cr/Al [IV] catalysts by DRIFTS. Additional measurements were done for the calcined 7.5Cr/Al catalyst and for the pure chromia and alumina samples. Figure 8 shows DRIFT spectra measured for the calcined or prereduced 13.5Cr/Al catalyst during isobutane dehydrogenation, and Figure 9 the Raman spectra measured for the calcined 13.5Cr/Al catalyst during propane dehydrogenation. The dehydrogenated alkane did not influence the type of species formed.

During the first minutes on alkane stream, formates and carboxylates formed after calcination with simultaneous disappearance of the chromate band, and carboxylates formed after hydrogen or carbon monoxide prereduction, although less rapidly than after calcination. The carbon-containing species present on the carbon monoxide-prereduced surface were not stable under the alkane atmosphere [IV]. For calcined catalysts, the carboxylates changed with increasing chromium content of the sample from alumina-bonded species to mostly chromia-bonded [IV]. The results suggested that the carboxylates were formed by at least two reactions: the reduction of Cr<sup>6+</sup> (and Cr<sup>5+</sup>) on the calcined catalyst by the alkane, and probably the reaction of gaseous hydrocarbons with surface hydroxyl groups [III, IV, 64, 65].

Hydrocarbon-type deposits formed gradually with simultaneous decrease in the dehydrogenation activity suggesting that these species contributed to the deactivation. Aliphatic species were formed first and unsaturated/aromatic and graphite-like species with increasing time on stream [III, IV, 50]. The gradual change to coke deposits that contained less hydrogen was in accordance with the decrease in the H/C ratio of coke with time on stream observed in the activity measurements [IV]. Prereduction of the chromia/alumina catalyst influenced the quantity but not the quality of the hydrocarbon-type species formed. Hydrogen decreased the formation of the aliphatic species but did not influence the unsaturated/aromatic or graphite-like species notably, whereas carbon monoxide increased the formation of the aliphatic and the unsaturated/aromatic species. This was in accordance with the activity measurements at 580 °C, where the carbon monoxide-prereduced surface contained the highest amount of coke.

The hydrocarbon-type deposits were most likely formed from adsorbed dehydrogenation intermediates or products (alkenes) [III, IV, 50, 66], which agrees with the general notion that alkenes are more reactive to coke formation than alkanes [67]. Based on the gradual change observed in the nature of the carbon-containing deposits, polymerisation, cyclisation and dehydrogenation reactions of these species took place with increasing amount and age of the coke. The chromia and the alumina phases were both involved in coke formation [IV, 32]. Active sites for coke formation may have been Lewis acidic cations [68] or Brønsted acidic hydroxyl species [67]. On the Lewis acid sites the formation of coke from alkenes has been proposed to take place via allylic intermediate species [68]. However, in general the formation of carbonaceous deposits on oxide catalysts is thought to occur on Brønsted acid sites as a result of cracking reactions involving coke precursors [67]: carbocation intermediates are formed on the acid sites and undergo dehydrogenation (polymerisation) and cyclisation reactions leading to aromatic species, which react further to higher molecular weight polynuclear aromatics and condense as coke. The alumina-bonded hydroxyls detected by DRIFTS during dehydrogenation, although weakly acidic, possibly contributed to the cracking of the alkanes [64], also, observed as another side reaction.

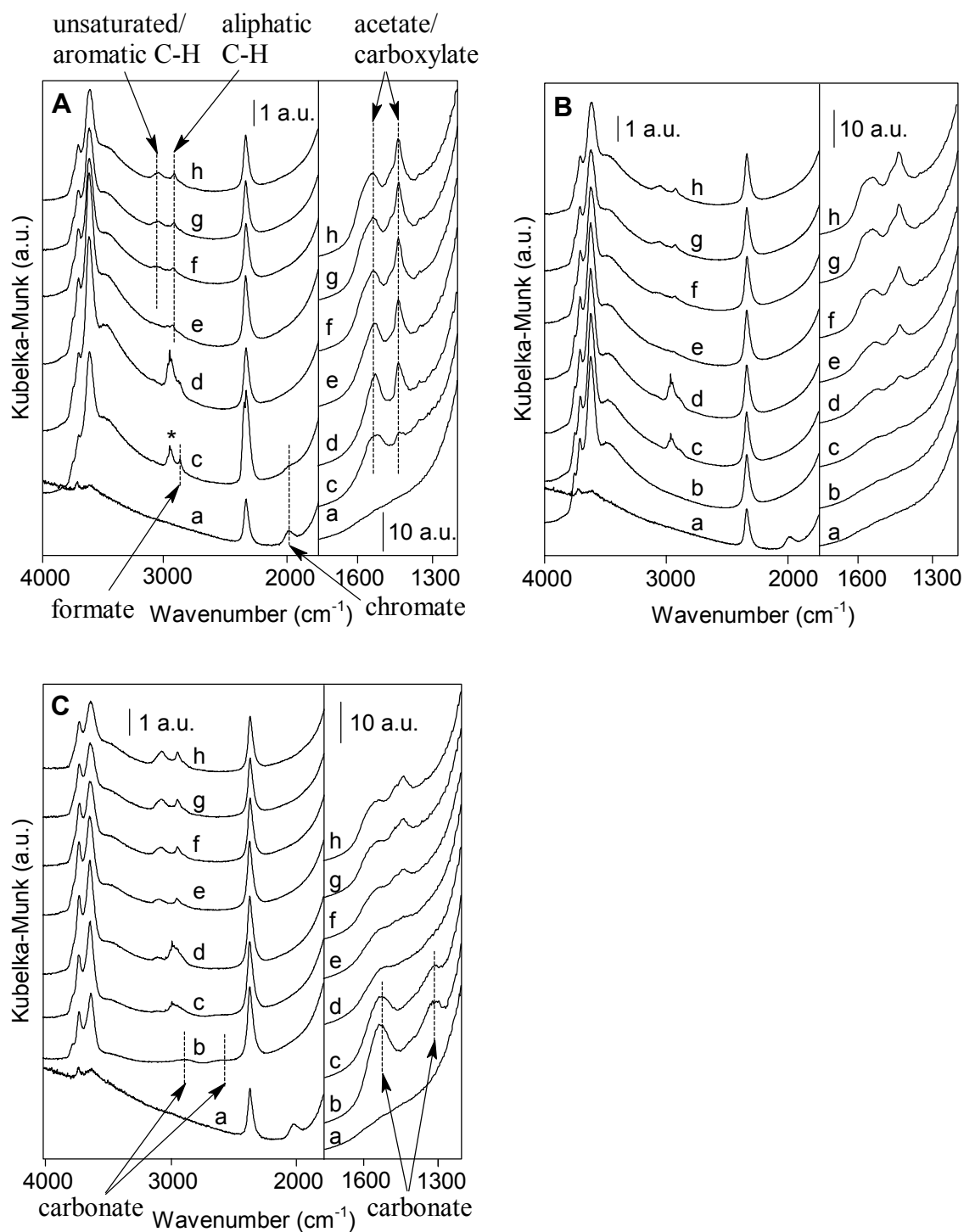


**Figure 8.** DRIFT spectra measured for (A) calcined, (B)  $\text{H}_2$ -prereduced and (C)  $\text{CO}$ -prereduced 13.5Cr/Al catalyst at 580  $^{\circ}\text{C}$  (a) after calcination, (b) after  $\text{H}_2$  or  $\text{CO}$  prereduction, and during the isobutane dehydrogenation measurement after (c) 10 s, (d) 1 min 10 s, (e) 3, (f) 6, (g) 10 and (h) 15 min on isobutane stream. Spectra (c) and (d) measured under isobutane flow and spectra (e)–(h) after nitrogen flush. \*Gaseous isobutane. [IV]

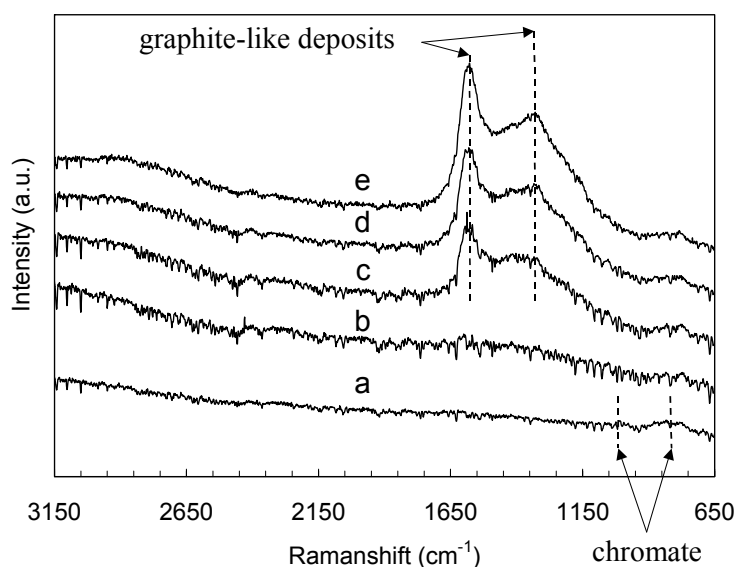


**Figure 9.** Raman spectra measured for the calcined 13.5Cr/Al catalyst at 580 °C (a) after calcination, and during the propane dehydrogenation measurement after (c) 10, (d) 20, (e) 30 and (f) 40 min on propane stream. Spectra measured after helium flush. [III]

#### 4.3.3. Considerations on the effect of prereduction

The lower dehydrogenation activity after hydrogen prereduction has been suggested to be related to a different structure or concentration of the OH/H groups formed during hydrogen prereduction compared to those on the alkane-reduced surface [21]. The quality of the hydroxyl groups is not the primary cause for the different activities because similar isolated and associated hydroxyl species were present on the hydrogen- and the alkane-reduced surfaces. The quantities of the different hydroxyl groups, or the presence of adsorbed hydrogen molecules or ions is probably more important, but exact comparison of the amounts of the different species is difficult. The total amount of “water” on the reduced surfaces can be estimated from the difference between the calculated and the detected amount of water produced during reduction of  $\text{Cr}^{6+}$  to  $\text{Cr}^{3+}$ . It is more difficult to determine the number of the individual hydroxyl species since the DRIFTS results do not allow their quantitative determination, and, moreover, on the alkane-reduced surface some of the hydrogen ions may be in the acetate and the aliphatic species instead of the hydroxyls.

On the other hand, the main difference observed by DRIFTS between the hydrogen- and the alkane-reduced surfaces was the more rapid formation of carboxylates and aliphatic species after calcination. This, combined with the higher activity after alkane reduction, could suggest the involvement of these species in the dehydrogenation reaction. However, they were not active sites for dehydrogenation since carboxylates formed also on the pure chromia and alumina samples, which had negligible dehydrogenation activities. Nijhuis et al. [66] suggested that the coke layer formed on chromia/alumina during propane dehydrogenation could facilitate the adsorption of alkane on the catalyst and, in this way, explain the increase in activity they observed with increasing amount of coke with time on stream. However, this explanation seems intuitively less probable than the OH/H proposal discussed above: in the present experiments the activity of the catalysts decreased continuously with time on stream. Furthermore, the less extensive coke formation observed for the hydrogen-prereduced surface and, thus, its slower deactivation may simply have been related to the lower initial dehydrogenation activity of the surface.

Several explanations have been proposed for the difference in the dehydrogenation behaviour between the alkane-reduced and the carbon monoxide-prereduced surfaces. The absence of OH/H species and presence of carbonaceous deposits on the carbon monoxide-prereduced surface have been postulated as possible causes, as has also reduction of  $\text{Cr}^{6+}$  or  $\text{Cr}^{5+}$  by carbon monoxide to  $\text{Cr}^{2+}$ , unselective in dehydrogenation [21]. The involvement of  $\text{Cr}^{2+}$  cannot be confirmed or ruled out based on the present results. However, it seems acceptable that both the higher number of c.u.s. chromium sites and the carbon-containing species present on the carbon monoxide-prereduced surface contributed to the lower activity in dehydrogenation and the more extensive coke formation. The additional c.u.s. sites were possibly more selective for the side reactions than for dehydrogenation, and the carbonate and formate species may have acted as coke precursors.

Clustering of the chromia phase during reduction might also influence the catalytic activity of chromia/alumina. This could take place by two ways: (i) by the decrease in the number of active sites with increase in the size of three-dimensional chromia

clusters, or (ii) by the more significant contribution of the alumina support to cracking and coke formation with increase in the area of exposed alumina surface. These phenomena might contribute to the different behaviour of the reduced samples in dehydrogenation if the extent of clustering was different. According to the results, clustering may have taken place during reduction of the 13.5Cr/Al catalyst. However, it is unclear whether the extent of clustering varied on the samples reduced with different gases.

#### **4.4 Deactivation of ALD-prepared and fluidised bed chromia/alumina**

The dehydrogenation behaviour of the ALD-prepared 13.5Cr/Al catalyst was compared with the FB1 catalyst developed for fluidised bed operation [V]. The samples were studied in cycles of (pre)reduction–dehydrogenation–regeneration and by repeated oxidation–H<sub>2</sub>-TPR experiments to investigate differences in activity and deactivation. In industrial operation, the deactivation of chromia/alumina takes place in three time scales [69]. In short time scale the catalyst deactivates during a single dehydrogenation stage with time on stream due to coke formation. In longer time scale, the deactivation takes place in cycles of dehydrogenation–regeneration: in medium term as the activity of a fresh catalyst decreases to a stable operating level, and in long term during several months as more extensive structural changes occur. The changes investigated here refer to the “short” and “medium” term deactivation.

##### **4.4.1 Behaviour with time on alkane stream**

The activities of the samples were investigated in 12 cycles of (prereduction)–dehydrogenation–regeneration. Cycles 7–11 included a prereduction stage with hydrogen whereas cycles 1–6 and 12 did not. Figure 10 shows the activities of the samples during one 15 min isobutane dehydrogenation stage after prereduction by hydrogen (data from cycle 7). The overall behaviour was similar after calcination.

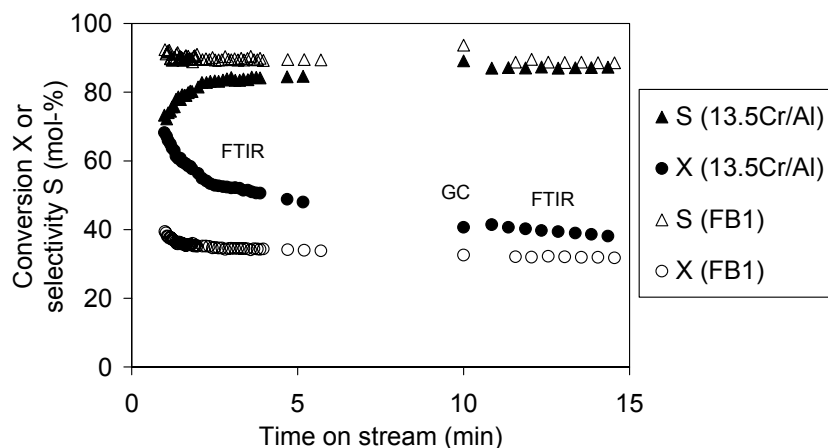


**Figure 10.** Conversion of isobutane (X) and selectivity to isobutene (S) for the 13.5Cr/Al and FB1 catalysts in dehydrogenation of isobutane at 580 °C, 1.03 bar, WHSV 15 h<sup>-1</sup> and nitrogen dilution 1 mol/1 mol. [V]

The 13.5Cr/Al catalyst was more active than the FB1 catalyst but the initial selectivity to isobutene was lower due to high cracking activity. In addition, the 13.5Cr/Al catalyst deactivated more rapidly with increase in selectivity to isobutene. The coke contents of the 13.5Cr/Al and FB1 samples were 3.8 and 0.7 mmol<sub>C</sub>/g<sub>cat</sub>, respectively, after the dehydrogenation stage.

It was suggested in publication V that the high dehydrogenation and coking activity of the 13.5Cr/Al sample was due to its higher redox Cr<sup>3+</sup> site content, implying that redox Cr<sup>3+</sup> would be more active in dehydrogenation but less selective than non-redox Cr<sup>3+</sup>. However, the surface areas of the catalysts were not considered. Taking these into account—166 and 63 m<sup>2</sup>/g for the 13.5Cr/Al and FB1 samples, respectively—the corresponding chromium atom loadings per sample unit surface area were 9.4 and 22.1 at<sub>Cr</sub>/nm<sup>2</sup><sub>sample</sub>, and the Cr<sup>6+</sup> contents were 2.0 and 1.8 at<sub>Cr</sub>/nm<sup>2</sup><sub>sample</sub>. Thus, the surface density of Cr<sup>6+</sup> was quite similar for the two samples, as would be expected on the basis of Figure 1. The difference in the initial dehydrogenation activity was most likely related to the total chromium densities. For the 13.5Cr/Al catalyst this coincided with the range where the highest activity in dehydrogenation occurs, 8–9 at<sub>Cr</sub>/nm<sup>2</sup>, whereas for the FB1 catalyst it was significantly higher. Therefore, the FB1 catalyst most likely

contained a higher number of unexposed  $\text{Cr}^{3+}$  sites inactive in dehydrogenation. This would explain why this catalyst was less active in dehydrogenation than the 13.5Cr/Al catalyst, even though their chromium contents were comparable in weight percent (Table 2). Moreover, the supports of the catalysts may have contributed to the different dehydrogenation behaviours. Although the alumina used in the FB1 catalyst was unknown, it is likely it was not the same as the one used in the 13.5Cr/Al catalyst.

The in situ spectroscopic measurements indicated that hydrocarbon-type coke is formed during alkane dehydrogenation primarily from adsorbed dehydrogenation intermediates/products and deactivates the catalyst [III, IV]. Therefore, it seems that the more pronounced coke formation, and thus the rapid deactivation of the 13.5Cr/Al catalyst compared to the FB1 catalyst was related to the high initial activity of the ALD-prepared catalyst. Its higher cracking activity may have increased coke formation also. The exposed alumina surface present under dehydrogenation conditions indicated by the reduction measurements most likely contributed to both side reactions.

The DRIFTS results and those described above support the suggestion that a high chromium surface density is beneficial for the dehydrogenation stability, although it decreases the initial activity. It seems that uncovered alumina support decreases the selectivity stability of chromia/alumina in dehydrogenation. Potassium used as promoter in these catalysts has been claimed to neutralise the unselective alumina acid sites. Another approach would be to cover the alumina with the chromia phase. Even though the 13.5Cr/Al catalyst contained chromium twice the amount required for the so-called monolayer coverage,  $8.0 \text{ at}_{\text{Cr}}/\text{nm}^2_{\text{support}}$  compared to about  $4\text{--}5 \text{ at}_{\text{Cr}}/\text{nm}^2$ , some of the alumina surface was still exposed. Apparently, significantly more chromium is required to keep the surface of the support fully covered under reaction conditions. At the same time the chromia phase should remain amorphous since crystalline  $\alpha\text{-Cr}_2\text{O}_3$  is known to lower the dehydrogenation activity.

#### 4.4.2 Behaviour in cycles of (pre)reduction–dehydrogenation–regeneration

The deactivation and the structural changes of the chromia/alumina catalysts in longer time scale was investigated with the 12 isobutane dehydrogenation–regeneration cycles (Figure 11) and with the repeated oxidation–H<sub>2</sub>-TPR measurements (Figure 12).

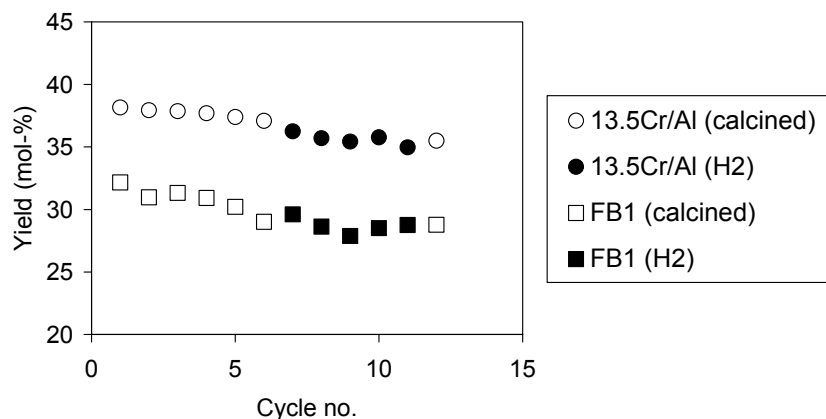


**Figure 11.** Yield of isobutene in 12 consecutive isobutane dehydrogenation stages for the 13.5Cr/Al and FB1 catalysts after calcination or H<sub>2</sub> prereduction at 10 min on isobutane stream at 580 °C, 1.03 bar, WHSV 15 h<sup>-1</sup> and nitrogen dilution 1 mol/1 mol. [V]

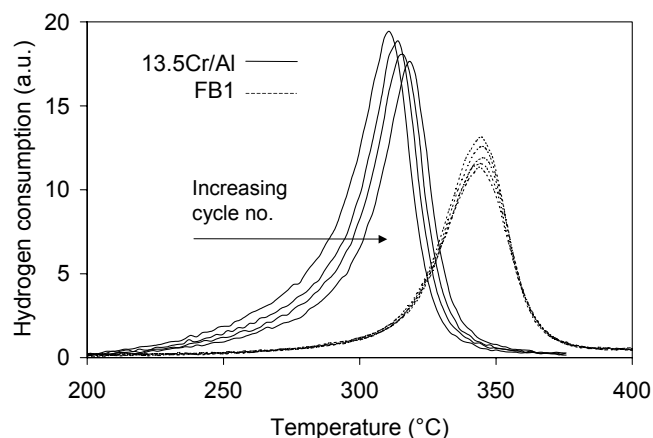


**Figure 12.** TPR profiles for the 13.5Cr/Al and FB1 catalysts in repeated oxidation–H<sub>2</sub>-TPR cycles. [V]

During the 12 cycles the two catalysts showed almost similar deactivation behaviour, the FB1 catalyst deactivating slightly faster. FTIR gas analysis measurements and the repeated H<sub>2</sub>-TPR experiments indicated a decrease in the amount of reducible Cr<sup>6+</sup> sites with cycling with the decrease being more significant for the 13.5Cr/Al than for the FB1 catalyst.

Examination of the TPR results revealed differences between the properties of the reducible sites and, thus in the structures of the catalysts. The single-peak shape of the TPR profiles indicated that one dominant reduction process was occurring on both catalysts, most likely Cr<sup>6+</sup> reducing to Cr<sup>3+</sup>. Otherwise, the TPR studies suggested differences between the catalysts. First, the reducible sites on the FB1 sample were on average more difficult to reduce, indicating that they were in stronger interaction with their surroundings. Second, the sites on the FB1 catalyst appeared to be more homogeneous in nature, whereas the 13.5Cr/Al catalyst contained a more heterogeneous mixture of chromium species with different reducibilities [37]. The kinetic modelling of the TPR patterns [V, 37] suggested further differences between the catalysts. In the modelling of TPR patterns, the reduction process is assumed to take place through two stages: formation of germ nuclei and the growth of these nuclei [70]. The nucleation seemed to occur less readily on the FB1 catalyst than on the 13.5Cr/Al catalyst.

In the repeated H<sub>2</sub>-TPR experiments the temperature at which the reduction rate reached its maximum ( $T_{\max}$ ) increased with cycling for the 13.5Cr/Al catalyst, whereas for the FB1 catalyst it remained practically constant. This suggested that the structure of the reducible sites was less stable on the ALD-prepared catalyst. It is possible that on the FB1 catalyst mainly the number of these sites decreased, whereas on the 13.5Cr/Al catalyst not only the number but also the average structure changed. Taking into account the TPR results and the significantly different surface chromium loadings of these samples, it is clear that the surface structures of these catalysts were different. For example, the FB1 catalyst most likely contained more Cr<sup>6+</sup> located on top of the chromia phase, whereas on the ALD catalyst some Cr<sup>6+</sup> may still have been interacting with the alumina support, which would explain their more heterogeneous nature.

The deactivation of the catalysts was attributed to the decrease in the number of redox  $\text{Cr}^{3+}$  sites with cycling [V], in accordance with Hakuli et al. [25]. However, since also non-redox  $\text{Cr}^{3+}$  is active in dehydrogenation [I, 25, 26], a decrease in the total number of redox and non-redox sites must have contributed to the deactivation. Three possible phenomena may have contributed to the loss of active chromium: (i) clustering (sintering) of the active phase to three-dimensional structures during reduction/dehydrogenation [25, 71, 72], (ii) migration of  $\text{Cr}^{3+}$  into the alumina lattice [19] and (iii) encapsulation of chromium inside the alumina support as the surface of the alumina collapses [31].

Hakuli et al. [25] attributed the decrease in the number of active sites (according to them mainly redox  $\text{Cr}^{3+}$ ) rather to the irreversible clustering of the chromium species during reduction than to the migration of the active sites into the alumina lattice. Investigations on the reduction of the 13.5Cr/Al catalyst suggested that chromia species might indeed cluster during reduction [II–IV]. The increase in the amount of reducible chromium observed after longer oxidation times may support this; it is possible that clustered species were better redispersed if oxidised for a longer time. In addition, the  $T_{\text{max}}$  shift in the TPR measurements with the 13.5Cr/Al catalyst possibly indicates that the reducible species were more mobile on this catalyst and, thus, more susceptible to the clustering. It has been proposed by Buonomo et al. [73] that a stable structure of the active phase is beneficial for dehydrogenation behaviour. The authors described a potassium-promoted chromia/alumina dehydrogenation catalyst where the active phase had high dispersion and homogeneous distribution, and had been fixed in this position by a lattice of oligomeric silicon dioxide. They proposed the fixing to prevent the active phase from crystallising and to ensure high activity, mechanical strength and stability.

Other causes for the irreversible deactivation include the migration or the encapsulation of the chromium species inside alumina. Chromium has been detected to migrate into the alumina framework when chromia/alumina samples are treated at high temperatures, generally above 800 °C [19, 31]. This process takes place in industrial conditions over several months, where during regeneration the temperature increases significantly due to the exothermal coke combustion, leading to formation of a solid solution of chromia

and alumina [11]. The encapsulation, on the other hand, occurs as the surface structure of alumina collapses [31] and, presumably, also requires elevated temperatures to occur extensively. It seems unlikely that either of these processes took place in a significant degree in the time scale and reaction conditions used in publication V. The highest temperature increase observed during reduction or regeneration was 15 °C meaning that the temperature did not exceed 610 °C at any point.

It remains of interest why the two catalysts appeared to deactivate at almost similar rates—or the FB1 catalyst even slightly faster—even though the number of redox  $\text{Cr}^{3+}$  sites on the 13.5Cr/Al catalyst decreased faster and the catalyst was more unstable. The first point is explained by the activity of both redox and non-redox  $\text{Cr}^{3+}$  in dehydrogenation. Regarding the difference in the stabilities of the catalysts, it might be that on the ALD-prepared catalyst the active species not only clustered but also redispersed more easily. In this case, even though the number of redox sites would have decreased faster, the irreversible decrease in the number of all active sites could have been less extensive. This might have occurred, also, if some of the former redox sites remaining in oxidation state +3 formed active non-redox species. Moreover, it is likely that on the FB1 sample the surface stabilisation process took place on a smaller scale and was rapid at first but then slowed down. With the FB2 catalyst, which was similar to the FB1 sample, the number of redox  $\text{Cr}^{3+}$  sites and the activity in isobutane dehydrogenation stabilised after about 16 cycles of (pre)reduction–dehydrogenation–regeneration [VI]. With the ALD-prepared catalyst the stabilisation of the mobile surface species probably would have taken a longer time.

#### **4.5 Kinetic model for isobutane dehydrogenation**

A kinetic model was derived for the dehydrogenation reaction [VI]. For modelling purposes, the activity of the FB2 catalyst was measured under different reaction conditions at 520–580 °C and 1.03 bar. After an initial deactivation period the activity of the catalyst stabilised both with time on isobutane stream and also in series of several (pre)reduction–dehydrogenation–regeneration cycles. Therefore, it was not necessary to include deactivation factors into the kinetic models.

Twelve kinetic models were evaluated to describe the dehydrogenation reaction: a simple power law model, eight models derived from four different dehydrogenation mechanisms and three models proposed earlier by other authors [74–76]. In the derivation of the mechanism-based models, the reaction rate-determining step (RDS) was assumed to be either the adsorption of isobutane or the surface reaction, that is the abstraction of hydrogen from the adsorbed species. The mechanisms described in detail in publication VI had two main variables: (i) the active site, which was assumed to be either a chromium ion or a pair of chromium and oxygen ions, and (ii) the total number of chromium ions required by the reaction, which varied between one and three.

The best fit between the measured and estimated compositions of the product stream was obtained with three mechanism-based models: one based on mechanism II (publication VI) assuming the adsorption of isobutane as the RDS, and two based on mechanism III assuming either the adsorption or the surface reaction as the RDS. Due to the similarities between the mathematical forms of the models and the results obtained, the equations could be simplified to the form presented in (7).

$$-r'_A = \frac{k' \left( p_A - \frac{p_E p_{H_2}}{K} \right)}{1 + K' p_E p_{H_2}^{1/2} + (K_{H_2} p_{H_2})^{1/2}} \quad (7)$$

However, the three best models described the reaction only slightly better than most of the other models tested. Based on the results it was possible to conclude which parameters were required in the rate equations for a satisfactory description. Usually the adsorption parameter of isobutane had a very low value or was less well determined than the other adsorption parameters, and could be omitted from the equations. On the other hand, the isobutene and hydrogen adsorption parameters were both required. Squaring the denominator of the equation, corresponding to the rate-determining step with two active sites, was not necessary. The simplest model studied to fulfil these requirements and to describe the reaction with a good accuracy is presented in equation (8). This model, with adsorption as the RDS, was proposed earlier by Happel et al. [74] for isobutane dehydrogenation on chromia/alumina.

$$-r'_A = \frac{k' \left( p_A - \frac{p_E p_{H_2}}{K} \right)}{1 + K_E p_E + K_{H_2} p_{H_2}} \quad (8)$$

The difference between the results obtained with the models presented in equations (7) and (8) was negligible (Figure 13). The parameter values estimated with the models were physically meaningful. The activation energy of the RDS was estimated to be  $141 \pm 3$  kJ/mol with equation (7) and  $142 \pm 3$  kJ/mol with equation (8). In general, the estimated activation energy was between 133 and 142 kJ/mol with the models assuming isobutane adsorption as the rate-determining step.

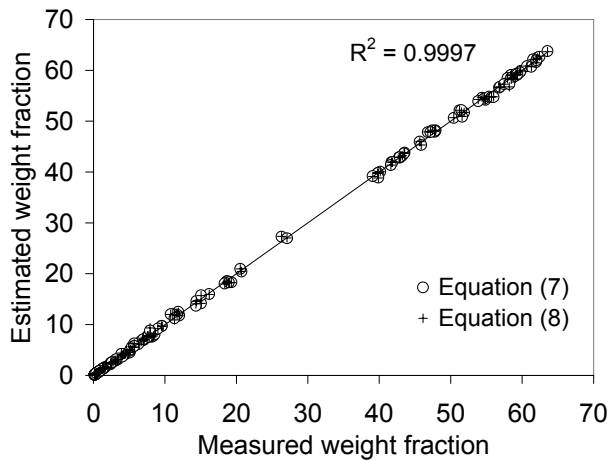
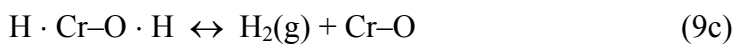


**Figure 13.** Correlation between the measured and estimated weight fractions in the product stream with equations (7) and (8). [VI]

The most descriptive mechanism of the four tested ones could not be determined conclusively. Intuitively the most probable one is presented below.



The mechanism takes into account the findings that the dehydrogenation activity increases linearly with the chromium content of the catalyst [19, 24–26], suggesting that only one chromium ion is needed for the reaction to occur, and that oxygen ions on the surface may take part in the reaction [I, 19, 39]. A similar reaction pathway for alkane dehydrogenation was earlier proposed by Weckhuysen and Schoonheydt [19]. However, the results did not support this mechanism better than the other three.

To conclude, kinetic modelling is a useful tool for obtaining models for the purposes of activity prediction and reactor design and scale-up. Fundamental mechanistic studies would, however, benefit from combining kinetic modelling with for example isotopic tracer or adsorption studies. Nevertheless, some general suggestions could be made about the mechanism for dehydrogenation. Since the isobutane adsorption term was not required in the models, the results supported the adsorption of isobutane as the rate-determining step. Furthermore, the rate-determining step seemed to require only one chromium ion, which agrees with the idea that the adsorption could occur by dissociation on a pair of chromium and oxygen ions. The involvement of surface oxygen ions in the reaction was supported also by the results obtained with the aluminium nitride-modified catalysts [I].

## 5 SUMMARY

The aim of this work was to obtain structure–activity information, which could be utilised in the optimisation of the dehydrogenation properties of chromia/alumina catalysts. Catalysts prepared by the atomic layer deposition method and those developed for fluidised bed operation were characterised by advanced ex situ and in situ techniques and their activities were measured in the dehydrogenation of light alkanes. The reduction, dehydrogenation behaviour and deactivation of chromia/alumina were investigated, including the mechanism of dehydrogenation, and a comparison was made between chromium catalysts prepared on alumina and aluminium nitride-modified alumina.

The common factor in all parts of the work was the active site for dehydrogenation; its structure and behaviour in the reaction. The dehydrogenation activity of chromia catalysts was attributed to coordinatively unsaturated redox and non-redox  $\text{Cr}^{3+}$  ions even at low chromium loadings. The reduction of the high oxidation state chromium ions by hydrogen and alkanes resulted in formation of hydroxyl groups bonded to chromia and alumina, and by carbon monoxide and alkanes in deposition of carbon-containing species. Prereduction of chromia/alumina affected its activity in dehydrogenation. The decrease in dehydrogenation activity caused by hydrogen prereduction was suggested to be related to the amount of OH/H species on the catalyst surface. Prereduction with carbon monoxide decreased the selectivity to dehydrogenation products, which was possibly caused by a higher number of unselective chromium sites on the reduced surface and by the carbonaceous species formed during prereduction.

The results obtained with the catalysts prepared on aluminium nitride-modified alumina suggested that the oxygen ions on the surface of chromia also participate in dehydrogenation. The reaction may start with a step where the isobutane molecule dissociates to a pair of chromium and oxygen ions. In the kinetic modelling of isobutane dehydrogenation, activity results were best described by a model assuming isobutane

adsorption, possibly on a Cr–O pair, as the rate-determining step. The activation energy for the reaction was estimated to be 133–142 kJ/mol.

The chromia/alumina catalysts deactivated with time on stream and in cycles of (pre)reduction–dehydrogenation–regeneration. The deactivation with time on stream was mainly caused by coke formation. The nature of the carbon-containing species depended on the time on stream. Carboxylates and aliphatic hydrocarbon species were formed during the initial stages of the reaction, and unsaturated/aromatic hydrocarbons and graphite-like deposits with increasing time on stream. The carboxylates were most likely formed in reduction of the catalyst and in reactions of gaseous hydrocarbons with surface hydroxyl species, and the hydrocarbon-type deposits from adsorbed dehydrogenation intermediates/products by polymerisation, cyclisation and dehydrogenation reactions. The deactivation in several dehydrogenation–regeneration cycles was caused by a decrease in the number of active sites. This decrease was most likely due to the clustering of the active phase into more three-dimensional structures.

Hydroxyl species of exposed alumina support may have contributed to the side reactions observed during dehydrogenation. Catalysts prepared on aluminium nitride-modified alumina were investigated as alternatives. However, the activity and selectivity increase sought for by this approach was not observed, as the catalysts were less active than those prepared on unmodified alumina due to the unfavourable effect of nitrogen.

Based on the results of this work and on earlier literature some properties of the optimal chromia/alumina catalysts and their active sites can be summarised. The active site for dehydrogenation seems to be a coordinatively unsaturated pair of chromium and oxygen ions. Both redox and non-redox Cr<sup>3+</sup> are active at all chromium loadings, provided that the chromium ions are exposed on the surface and not present inside the alumina support or a large chromia crystal. Furthermore, the activities of the two sites are not necessarily different. It remains unclear, though, whether the activity of the chromium ion is influenced by its nuclearity, that is whether the Cr<sup>3+</sup> exists as an isolated ion or in a cluster of chromium ions. However, at the optimal chromium loading level, 8–9 at<sub>Cr</sub>/nm<sup>2</sup>, most of the active chromium sites are probably located in clusters in close

interaction with other chromium ions. At the optimal loading some alumina still remains uncovered during dehydrogenation and may contribute to the side reactions taking place during dehydrogenation. Therefore, attention should be paid to the properties of the alumina support. Either the alumina should be modified or the chromium content should be increased so that the alumina surface would be totally covered. In the latter case the chromia phase should remain amorphous. When the chromia/alumina catalyst is prereduced before dehydrogenation, no alkane is consumed in the reduction. Prereduction of chromia/alumina with hydrogen appears to be more beneficial for the dehydrogenation behaviour than prereduction with carbon monoxide: the surface is more selective to dehydrogenation and deactivates less rapidly.

## NOMENCLATURE

### Symbols and abbreviations

AAS	atomic absorption spectroscopy
acac	acetyl acetonate ion, $C_5O_2H_7^-$
ALD	atomic layer deposition
ALE	atomic layer epitaxy
alumina	aluminium oxide, $Al_2O_3$
a.u.	arbitrary unit
BET	Brunauer–Emmett–Teller
chromia	chromium oxide, $CrO_x$ (in catalysts), $Cr_2O_3$ (bulk chromia)
c.u.s.	coordinatively unsaturated
DH	dehydrogenation
DRIFT	diffuse reflectance Fourier transform infrared (spectroscopy)
DRS	diffuse reflectance spectroscopy
ESR	electron spin resonance (spectroscopy)
FB, FBD	fluidised bed
FTIR	Fourier transform infrared (spectroscopy)
GC	gas chromatograph(y)
INAA	instrumental neutron activation analysis
IR	infrared
isobutane	2-methylpropane
isobutene	2-methylpropene
isooctane	2,2,4-trimethylpentane
$k'$	(apparent) reaction rate constant, $mol/(kg_{cat} \times s \times bar)$
$K$	reaction equilibrium constant, bar
$K_i$	adsorption equilibrium constant of component $i$ , $bar^{-1}$
$K'$	combined adsorption equilibrium constant
LEIS	low energy ion spectroscopy
MS	mass spectrometry, mass spectrometer
MTBE	methyl- <i>tert</i> -butyl ether (2-methoxy-2-methylpropane)
<i>n</i> -alkenes	1-butene, <i>cis</i> -2-butene, <i>trans</i> -2-butene

ODH	oxidative dehydrogenation
$p_i$	partial pressure of component $i$ , bar
$-r'_A$	reaction rate of isobutane, mol/(kg <sub>cat</sub> ×s)
RDS	rate-determining step
S	selectivity, mol-%
silica	silicon dioxide, SiO <sub>2</sub>
SSR	sum of squares of the residuals
T	temperature
TMA	trimethylaluminium, Al(CH <sub>3</sub> ) <sub>3</sub>
TP	temperature-programmed
TPR	temperature-programmed reduction
WHSV	weight hourly space velocity, h <sup>-1</sup>
X	conversion, mol-%
XAS	X-ray absorption spectroscopy
XPS	X-ray photoelectron spectroscopy
XRD	X-ray diffraction
Y	yield, mol-%
zirconia	zirconium dioxide, ZrO <sub>2</sub>

### **Subscripts**

A	isobutane
E	isobutene
max	maximum

## REFERENCES

1. Anon., CMAI: On-Purpose Propylene Production Will Increase Share Of Future Global Demand, *Oil&Gas J.* **102** (2004) No 22, 54–56.
2. Jebens, A. M., Fenelon, S., Sasano, T., CEH Marketing Research Report Butylenes, In *Chemical Economics Handbook-SRI International*, August 1998.
3. Bhasin, M. M., McCain, J. H., Vora, B. V., Imai, T., Pujadó, P. R., Dehydrogenation and Oxydehydrogenation of Paraffins to Olefins, *Appl. Catal., A: Gen.* **221** (2001) 397–419.
4. Tullo, A. H., Propylene on Demand, *Chem. Eng. News* **81** (2003) No 50, 15–16.
5. Anon., Report: New Propylene Production Technologies Hold Great Promise, *Oil&Gas J.* **102** (2004) No 8, 50–52.
6. Lichtblau, J., Goldstein, L., Gold, R., MTBE Issues Include Question Of All Oxygenate Mandates, *Oil&Gas J.* **102** (2004) No 12, 18–26.
7. Sloan, H. D., Birkhoff, M., Gilbert, M. F., Nurminen, M., Pyh lahti, A., Isooctane Production from C<sub>4</sub>'s as an Alternative to MTBE. Presented at the NPRA 2000 Annual Meeting, San Antonio, T, March 26–28, 2000, Paper AM-00-34.
8. Marchionna, M., Di Girolamo, M., High Quality Fuel Components from C<sub>4</sub> Hydrocarbons, *Proceedings of the DGMK Conference "C<sub>4</sub>-C<sub>5</sub> Hydrocarbons: Routes to Higher Value-Added Products"*, ed. S. Ernst, A. Jess, J. A. Lercher, M. Marchionna, P. Prinz, E. Schwab, Munich Germany 2004, pp. 125–136.
9. Aittamaa, J., Keskinen, K. I., Flowbat, Neste Oy, Porvoo, 1999.
10. Anon., Metathesis, Dehydro Fill Propylene Shortfall, *Chemical Week* **161** (1999) No 41, 41–42.
11. Buonomo, F., Sanfilippo, D., Trifir , F., Dehydrogenation of Alkanes, In *Handbook of Heterogeneous Catalysis*, Vol. 5, ed. G. Ertl, H. Kn zinger, J. Weitkamp, VCH, Weinheim 1997, pp. 2140–2151.
12. Atkins, M. P., Evans, G. R., Catalytic Dehydrogenation—A Review of Current Processes and Innovations, *Erd l Erdgas Kohle* **111** (1995) 271–274.
13. B lt, H., Zimmermann, H., Dehydrogenation Process for Propane and Isobutane, *Erd l Erdgas Kohle* **111** (1995) 90–93.
14. Anon., The Uhde STAR Process. Oxydehydrogenation of Light Paraffins to Olefins, <http://www.uhde.biz/cgi-bin/byteserver.pl/pdf/broschueren/>

- Oil\_Gas\_Refinery/The\_Uhde\_Star\_Process.pdf*, September 28, 2004.
15. Rønnekleiv, M., Hasselgård, P., Læg Reid, T., Dehydrogenation of Isobutane with a New Developed Platinum Catalyst, *Proceedings of the DGMK Conference "C<sub>4</sub> Chemistry – Manufacture and Use of C<sub>4</sub> Hydrocarbons,"* ed. W. Keim, B. Lücke, J. Weitkamp, Aachen Germany 1997, pp. 109–112.
  16. Anon., Propane Dehydrogenation, [http://www.sintef.no/units/chem/catalysis\\_oslo/pdh.htm](http://www.sintef.no/units/chem/catalysis_oslo/pdh.htm), April 4, 2002.
  17. Harlin, E., *Molybdenum and Vanadium Oxide Catalysts in the Dehydrogenation of Butanes*, Doctoral thesis, Helsinki University of Technology, Espoo, 2001, 57 p.
  18. Gates, B. C., *Catalytic Chemistry*, John Wiley & Sons, Singapore 1992, p. 323.
  19. Weckhuysen, B. M., Schoonheydt, R. A., Alkane Dehydrogenation over Supported Chromium Oxide Catalysts, *Catal. Today* **51** (1999) 223–232.
  20. Centeno, M. A., Debois, M., Grange, P., Platinum Aluminophosphate Oxynitride (Pt–AlPON) Catalysts for the Dehydrogenation of Isobutane to Isobutene, *J. Catal.* **192** (2000) 296–306.
  21. Hakuli, A., *Preparation and Characterization of Supported CrO<sub>x</sub> Catalysts for Butane Dehydrogenation*, Doctoral thesis, Helsinki University of Technology, Espoo, 1999, 48 p.
  22. Weckhuysen, B. M., Wachs, I. E., Schoonheydt, R. A., Surface Chemistry and Spectroscopy of Chromium in Inorganic Oxides, *Chem. Rev.* **96** (1996) 3327–3349.
  23. Hakuli, A., Kytökivi, A., Krause, A. O. I., Suntola, T., Initial Activity of Reduced Chromia/Alumina Catalyst in *n*-Butane Dehydrogenation Monitored by On-Line FT–IR Gas Analysis, *J. Catal.* **161** (1996) 393–400.
  24. Kytökivi, A., Jacobs, J.-P., Hakuli, A., Meriläinen, J., Brongersma, H. H., Surface Characteristics and Activity of Chromia/Alumina Catalysts Prepared by Atomic Layer Epitaxy, *J. Catal.* **162** (1996) 190–197.
  25. Hakuli, A., Kytökivi, A., Krause, A. O. I., Dehydrogenation of *i*-Butane on CrO<sub>x</sub>/Al<sub>2</sub>O<sub>3</sub> Catalysts Prepared by ALE and Impregnation Techniques, *Appl. Catal., A: Gen.* **190** (2000) 219–232.

26. Cavani, F., Koutyrev, M., Trifirò, F., Bartolini, A., Ghisletti, D., Iezzi, R., Santucci, A., Del Piero, G., Chemical and Physical Characterization of Alumina-Supported Chromia-Based Catalysts and Their Activity in Dehydrogenation of Isobutane, *J. Catal.* **158** (1996) 236–250.
27. Grzybowska, B., Sloczynski, J., Grabowski, R., Weislo, K., Kozłowska, A., Stoch, J., Zielinski, J., Chromium Oxide/Alumina Catalysts in Oxidative Dehydrogenation of Isobutane, *J. Catal.* **178** (1998) 687–700.
28. De Rossi, S., Casaletto, M. P., Ferraris, G., Cimino, A., Minelli, G., Chromia/Zirconia Catalysts with Cr Content Exceeding the Monolayer. A Comparison with Chromia/Alumina and Chromia/Silica for Isobutane Dehydrogenation, *Appl. Catal., A: Gen.* **167** (1998) 257–270.
29. Cherian, M., Rao, M. S., Hirt, A. M., Wachs, I. E., Deo, G., Oxidative Dehydrogenation of Propane over Supported Chromia Catalysts: Influence of Oxide Supports and Chromia Loading, *J. Catal.* **211** (2002) 482–495.
30. Weckhuysen, B. M., Bensalem, A., Schoonheydt, R. A., In Situ UV–VIS Diffuse Reflectance Spectroscopy–On-line Activity Measurements. Significance of Cr<sup>n+</sup> species ( $n=2, 3$  and 6) in *n*-Butane Dehydrogenation Catalyzed by Supported Chromium Oxide Catalysts, *J. Chem. Soc., Faraday Trans.* **94** (1998) 2011–2014.
31. Puurunen, R. L., Weckhuysen, B. M., Spectroscopic Study on the Irreversible Deactivation of Chromia/Alumina Dehydrogenation Catalysts, *J. Catal.* **210** (2002) 418–430.
32. Gorriz, O. F., Cortés Corberán, V., Fierro, J. L. G., Propane Dehydrogenation and Coke Formation on Chromia–Alumina Catalysts: Effect of Reductive Pretreatments, *Ind. Eng. Chem. Res.* **31** (1992) 2670–2674.
33. Greenwood, N. N., Earnshaw, A., *Chemistry of the Elements*, Butterworth Heinemann, Great Britain 1997, pp. 1004–1007.
34. Brückner, A., Radnik, J., Hoang, D.-L., Lieske, H., In Situ Investigation of Active Sites in Zirconia-Supported Chromium Oxide Catalysts during the Aromatization of *n*-Octane, *Catal. Lett.* **60** (1999) 183–189.
35. Vuurman, M. A., Hardcastle, F. D., Wachs, I. E., Characterization of CrO<sub>3</sub>/Al<sub>2</sub>O<sub>3</sub> Catalysts under Ambient Conditions: Influence of Coverage and Calcination Temperature, *J. Mol. Catal.* **84** (1993) 193–205.

36. Lugo, H. J., Lunsford, J. H., The Dehydrogenation of Ethane over Chromium Catalysts, *J. Catal.* **91** (1985) 155–166.
37. Kanervo, J. M., Krause, A. O. I., Characterisation of Supported Chromium Oxide Catalysts by Kinetic Analysis of H<sub>2</sub>-TPR Data, *J. Catal.* **207** (2002) 57–65.
38. Trunschke, A., Hoang, D. L., Radnik, J., Lieske, H., Influence of Lanthana on the Nature of Surface Chromium Species in La<sub>2</sub>O<sub>3</sub>-Modified CrO<sub>x</sub>/ZrO<sub>2</sub> Catalysts, *J. Catal.* **191** (2000) 456–466.
39. De Rossi, S., Ferraris, G., Fremiotti, S., Garrone, E., Ghiotti, G., Campa, M. C., Indovina, V., Propane Dehydrogenation on Chromia/Silica and Chromia/Alumina Catalysts, *J. Catal.* **148** (1994) 36–46.
40. Burwell, Jr., R. L., Littlewood, A. B., Cardew, M., Pass, G., Stoddart, C. T. H., Reactions between Hydrocarbons and Deuterium on Chromium Oxide Gel. I. General, *J. Am. Chem. Soc.* **82** (1960) 6272–6280.
41. Resasco, D. E., Haller, G. L., Catalytic Dehydrogenation of Lower Alkanes, *Catalysis* **11** (1994) 379–411.
42. Puurunen, R. L., *Preparation by Atomic Layer Deposition and Characterisation of Catalyst Supports Surfaced with Aluminium Nitride*, Doctoral thesis, Helsinki University of Technology, Espoo, 2002, 78 p.
43. Haukka, S., Determination of Chromium in Catalysts by Ultraviolet/Visible Spectrophotometry, *Analyst* **116** (1991) 1055–1057.
44. Guerrero-Pérez, M. O., Bañares, M. A., Operando Raman–GC Studies of Alumina-Supported Sb-V-O Catalysts and Role of the Preparation Method, *Catal. Today* **96** (2004) 265–272.
45. Hakuli, A., Kytökivi, A., Lakomaa, E.-L., Krause, O., FT-IR in the Quantitative Analysis of Hydrocarbon Mixtures, *Anal. Chem.* **67** (1995) 1881–1886.
46. Aittamaa, J., Keskinen, K. I., Kinfitt, Laboratory of Chemical Engineering, Helsinki University of Technology, Espoo, 2001.
47. Kwon, H., Choi, S., Thompson, L. T., Vanadium Nitride Catalysts: Synthesis and Evaluation for n-Butane Dehydrogenation, *J. Catal.* **184** (1999) 236–246.
48. Kytökivi, A., Rautiainen, A., Root, A., Reaction of Acetylacetone Vapour with  $\gamma$ -Alumina, *J. Chem. Soc., Faraday Trans.* **93** (1997) 4079–4084.

49. Józwiak, W. K., Dalla Lana, I. G., Interactions Between the Chromium Oxide Phase and Support Surface; Redispersion of  $\alpha$ -Chromia on Silica, Alumina and Magnesia, *J. Chem. Soc., Faraday Trans.* **93** (1997) 2583–2589.
50. Airaksinen, S. M. K., Krause, A. O. I., Formation of Carbon-Containing Deposits on Chromia/Alumina during Isobutane Dehydrogenation, *Proceedings of the DGMK Conference "C<sub>4</sub>-C<sub>5</sub> Hydrocarbons: Routes to Higher Value-Added Products"*, ed. S. Ernst, A. Jess, J. A. Lercher, M. Marchionna, P. Prinz, E. Schwab, Munich Germany 2004, pp. 69-75.
51. Ilieva, L. I., Andreeva, D. H., Investigation of the Chromium Oxide System by Means of Temperature-Programmed Reduction, *Thermochim. Acta* **265** (1995) 223–231.
52. Weckhuysen, B. M., Schoonheydt, R. A., Jehng, J.-M., Wachs, I. E., Cho, S. J., Ryoo, R., Kijlstra S., Poels, E., Combined DRS–RS–EXAFS–XANES–TPR Study of Supported Chromium Catalysts, *J. Chem. Soc., Faraday Trans.* **91** (1995) 3245–3253.
53. Grünert, W., Saffert, W., Feldhaus, R., Anders, K., Reduction and Aromatization Activity of Chromia–Alumina Catalysts. I. Reduction and Break-in Behaviour of a Potassium-Promoted Chromia–Alumina Catalyst, *J. Catal.* **99** (1986) 149–158.
54. Busca, G., The Surface Acidity of Solid Oxides and Its Characterization by IR Spectroscopic Methods. An Attempt at Systematization, *Phys. Chem. Chem. Phys.* **1** (1999) 723–736.
55. Knözinger, H., Ratnasamy, P., Catalytic Aluminas: Surface Models and Characterization of Surface Sites, *Catal. Rev.–Sci. Eng.* **17** (1978) 31–70.
56. Morterra, C., Magnacca, G., A Case Study: Surface Chemistry and Surface Structure of Catalytic Aluminas, as Studied by Vibrational Spectroscopy of Adsorbed Species, *Catal. Today* **27** (1996) 497–532.
57. Busca, G., Fourier Transform-Infrared Spectroscopic Study of the Adsorption of Hydrogen on Chromia and on Some Metal Chromites, *J. Catal.* **120** (1989) 303–313.
58. Ballinger, T. H., Yates, Jr., J. T., IR Spectroscopic Detection of Lewis Acid Sites on Al<sub>2</sub>O<sub>3</sub> Using Adsorbed CO. Correlation with Al–OH Groups Removal, *Langmuir* **7** (1991) 3041–3045.

59. Davydov, A. A., *Infrared Spectroscopy of Adsorbed Species on the Surface of Transition Metal Oxides*, John Wiley & Sons, Chichester 1984, p. 148.
60. Turek, A. M., Wachs, I. E., DeCanio, E., Acidic Properties of Alumina-Supported Metal Oxide Catalysts: An Infrared Spectroscopic Study, *J. Phys. Chem.* **96** (1992) 5000–5007.
61. Bensalem, A., Weckhuysen, B. M., Schoonheydt, R. A., Nature of Adsorbed Species During the Reduction of CrO<sub>3</sub>/SiO<sub>2</sub> with CO. In situ FTIR Spectroscopic Study, *J. Chem. Soc., Faraday Trans.* **93** (1997) 4065–4069.
62. Hadjiivanov, K., Busca, G., Surface Chemistry of Oxidized and Reduced Chromia: A Fourier Transform Infrared Spectroscopic Study, *Langmuir* **10** (1994) 4534–4541.
63. Busca, G., Finocchio, E., Lorenzelli, V., Ramis, G., Baldi, M., IR Studies on the Activation of C–H Hydrocarbon Bonds on Oxidation Catalysts, *Catal. Today* **49** (1999) 453–465.
64. Ermini, V., Finocchio, E., Sechi, A., Busca, G., Rossini, S., An FTIR and Flow Reactor Study of the Conversion of Propane on  $\gamma$ -Al<sub>2</sub>O<sub>3</sub> in Oxygen-Containing Atmosphere, *Appl. Catal., A: Gen.* **190** (2000) 157–167.
65. Datka, J., Eischens, R. P., Infrared Study of Coke on Alumina and Zeolite, *J. Catal.* **145** (1994) 544–550.
66. Nijhuis, T. A., Tinnemans, S. T., Visser, T., Weckhuysen, B. M., Towards Real-Time Spectroscopic Process Control for the Dehydrogenation of Propane over Supported Chromium Oxide Catalysts, *Chem. Eng. Sci.* **59** (2004) 5487–5492.
67. Bartholomew, C. H., Mechanisms of Catalyst Deactivation, *Appl. Catal., A: Gen.* **212** (2001) 17–60.
68. Trombetta, M., Busca, G., Rossini, S. A., Piccoli, V., Cornaro, U., FTIR Studies on Light Olefin Skeletal Isomerization Catalysis. I. The Interaction of C<sub>4</sub> Olefins and Alcohols with pure  $\gamma$ -Alumina, *J. Catal.* **168** (1997) 334–348.
69. Gussow, S., Whitehead, R., Isobutane Dehydrogenation by Catofin as Feed for Motor Fuel Ether. Presented at the NPRA 1991 Annual Meeting, San Antonio, T, March 17–19, 1991, Paper AM-91-54.

70. Kanervo, J. M., Krause, A. O. I., Kinetic Analysis of Temperature-Programmed Reduction: Behavior of a  $\text{CrO}_x/\text{Al}_2\text{O}_3$  Catalyst, *J. Phys. Chem., B.* **105** (2001) 9778–9784.
71. Peña, J. A., Monzón, A., Santamaría, J., Fierro, J. L. G., Coking Kinetics of Fresh and Thermally Aged Commercial  $\text{Cr}_2\text{O}_3/\text{Al}_2\text{O}_3$  Catalyst, *Appl. Catal., A: Gen.* **101** (1993) 185–198.
72. Sterligov, O. D., Gitis, K. M., Slovetskaya, K. I., Shpiro, E. S., Rubinstein, A. M., Minachev, Kh. M., The Role of Chemical and Structural Changes on the Surface in Deactivation of Chromia–Alumina Catalysts in Dehydrogenation of Paraffinic Hydrocarbons, *Stud. Surf. Sci. Catal.* **6** (1980) 363–374.
73. Buonomo, F., Jezzi, R., Notari, B., Kotelnikov, G., Michailov, K., Patanov, V., Method for the Preparation of a Catalyst for the Dehydrogenation of  $\text{C}_3\text{--C}_5$  Paraffins, *US Patent 4,746,643*, App. June 16, 1986, Acc. May 24, 1988.
74. Happel, J., Kamholz, K., Walsh, D., Strangio, V., Kinetics of the Isobutane–Isobutene–Hydrogen System Using Tracers, *Ind. Eng. Chem. Fundam.* **12** (1973) 263–267.
75. Zwahlen, A. G., Agnew, J. B., Isobutane Dehydrogenation Kinetics Determination in a Modified Berty Gradientless Reactor, *Ind. Eng. Chem. Res.* **31** (1992) 2088–2093.
76. Suzuki, I., Kaneko, Y., Dehydrogenation of Propane over Chromia–Alumina–Potassium Oxide Catalyst, *J. Catal.* **47** (1977) 239–242.

INDUSTRIAL CHEMISTRY PUBLICATION SERIES

- No. 1 Niemelä, M.,  
Catalytic reactions of synthesis gas. Part I: Methanation and CO Hydrogenation. 1992.
- No. 2 Niemelä, M.,  
Catalytic reactions of synthesis gas. Part II: Methanol carbonylation and homologation. 1993.
- No. 3 Saari, E.,  
Substituoitujen bentseenien hapen-, rikin- ja typenpoisto vedyllä. 1994.
- No. 4 Niemelä, M.,  
Catalytic reactions of synthesis gas. Part III: Determination of reaction kinetics. 1993.
- No. 5 Niemelä, M.,  
Catalytic reactions of synthesis gas. Part IV: Heterogeneous hydroformylation. 1994.
- No. 6 Perä, M.,  
Activated carbon as a catalyst support. 1995.
- No. 7 Halttunen, M.,  
Hydrocarbonylation of alcohols, carboxylic acids and esters. 1996.
- No. 8 Puurunen, R.,  
Trimetyylialumiinin ja ammoniakkin reaktiot alumiininitridin valmistuksessa: kirjallisuuskatsaus. 2000.
- No. 9 Reinius, H.,  
Activity and selectivity in hydroformylation: Role of ligand, substrate and process conditions. 2001.
- No. 10 Harlin, E.,  
Molybdenum and vanadium oxide catalysts in the dehydrogenation of butanes. 2001.
- No. 11 Viljava, T.-R.,  
From biomass to fuels: Hydrotreating of oxygen-containing feeds on a CoMo/Al<sub>2</sub>O<sub>3</sub> hydrodesulfurization catalyst. 2001.
- No. 12 Karinen, R.,  
Etherification of some C<sub>5</sub>-alkenes to fuel ethers. 2002.
- No. 13 Puurunen, R.,  
Preparation by atomic layer deposition and characterisation of catalyst supports surfaced with aluminium nitride. 2002.
- No. 14 Rautanen, P.,  
Liquid phase hydrogenation of aromatic compounds on nickel catalyst. 2002.
- No. 15 Pääkkönen, P.,  
Kinetic studies on the etherification of C<sub>5</sub>-alkenes to fuel ether TAME. 2003.
- No. 16 Kanervo, J.,  
Kinetic analysis of temperature-programmed reactions. 2003.
- No. 17 Lylykangas, M.,  
Kinetic modeling of liquid phase hydrogenation reactions. 2004.
- No. 18 Lashdaf, M.,  
Preparation and characterisation of supported palladium, platinum and ruthenium catalysts for cinnamaldehyde hydrogenation. 2004.